Modeling and Control of Low-Voltage DC Microgrid With Photovoltaic Energy Resources

by

Omar Alarfaj

A thesis
presented to the University of Waterloo
in fulfillment of the
thesis requirement for the degree of
Master of Applied Science
in
Electrical and Computer Engineering

Waterloo, Ontario, Canada, 2014

AUTHOR'S DECLARATION

I hereby declare that I am the sole author of this thesis. This is a true copy of the thesis, including any required final revisions, as accepted by my examiners.

I understand that my thesis may be made electronically available to the public.

Abstract

The use of DC microgrids is a promising concept that could improve power system reliability and stability in the future. The advantages of microgrids in general include an increase in energy efficiency through lowered energy transmission and operational costs, a reduced carbon footprint through the integration of renewable energy resources, and improvements in power quality and availability to end users through the use of advanced control techniques. DC microgrids have the potential to provide additional advantages, including decreasing interconnection conversion levels of distributed energy resources and energy storage systems, and preventing the propagation of power system disturbances.

Power system research groups around the world are investigating the DC microgrid concept through simulation platforms and experimental setups. Several strategies have been proposed for the control of DC microgrids, including hierarchical, distributed, and intelligent control strategies. In this work, PSCAD/EMTDC simulation environment was used for the modeling and simulation of a DC microgrid. A power management strategy was then implemented in order to ensure voltage regulation and seamless transition between grid-connected and isolated modes. The strategy is based on an autonomous distributed control scheme in which the DC bus voltage level is used as an indicator of the power balance in the microgrid. The autonomous control strategy does not rely on communication links or a central controller, resulting in reduced costs and enhanced reliability. As part of the control strategy, an adaptive droop control technique is proposed for PV sources in order to maximize the utilization of power available from these sources while ensuring acceptable levels of system voltage regulation. These goals are achieved by avoiding the curtailment of renewable energy until violation of the voltage regulation limit occurs. The adaptive droop control then curtails the output power of the PV sources and, at the same time, restores the DC voltage level to within an acceptable tolerance range.

Acknowledgements

All praise is due to Allah, the most beneficent, the most merciful, for guidance and help in all aspects of my life. All praise is due to Allah for giving me the ability to accomplish this work.

I would like to express my sincere appreciation and thanks to my advisor Professor Ehab El-Sadaany for his guidance, encouragement, and support through this work. Professor Ehab advices have drawn the path for me to step into the field of academic research.

I extend my thanks to my thesis committee members, Professor Tarek El-Fouly and Professor Shesha Jayaram for serving in my examination committee and for their valuable feedback.

I would like to thank my parents for their passion and continuous support throughout my life periods. Their ceaseless wishing for my development was the key driver for me to seek more achievements and higher status.

I am deeply grateful for my wife Asma for her overwhelming love and care. I owe Asma my deepest gratitude for her patience along this long journey to fulfill my goals. My children Jenan and Abdulrahman always bring the most joyful moments to my life even during most stressful times.

Special thanks to my colleagues Walied Alharbi, Bandar Alqahtani, Hasan Alrajhi, Mohamed Abdelwahed, and Majed Alotaibi for their support to overcome difficulties during my study.

Dedication

To my parents for their unconditional love and support,

To my family who gave color to my life.

Table of Contents

AUTHOR'S DECLARATION ii
Abstract iii
Acknowledgements iv
Dedication v
Table of Contents vi
List of Figures ix
List of Tables x
Chapter 1 Introduction 1
1.1 Motivation 1
1.2 Organization of Thesis 4
Chapter 2 Literature Review 5
2.1 DC Distribution System Configurations 5
2.2 DC Microgrid Control Strategies 7
2.2.1 Hierarchical Control 7
2.2.2 Distributed Control 9
2.2.2.1 Autonomous Distributed Control 9
2.2.2.2 Multi-agent Control 11
2.2.3 Intelligent Control 11
2.3 Solar Energy Sources 12
2.4 Energy Storage Systems 13
2.4.1 Electric Double-Layer Capacitors 13
2.4.2 Batteries 14
2.4.3 Flywheels 15
2.4.4 Superconducting Magnetic Energy Storage 16
2.5 Summary 16
Chapter 3 DC Microgrid System Model 19
3.1 CERTS Microgrid Test Bed Overview 19
3.2 Power System Component Sizing 20

3.2.1 Loads 20
3.2.2 Feeders 22
3.3 Energy Storage System Model 22
3.4 Solar Source Model 23
3.5 Summary 25
Chapter 4 Power Management Strategy 27
4.1 Control Strategy Objectives 27
4.2 Implemented Control Strategy 28
4.2.1 Grid-Side Converter Control 29
4.2.2 ESS Converter Control 30
4.2.3 DG Converter Control 31
4.3 Simulation Results 33
4.3.1 Normal System Operation 33
4.3.2 Step Load Changes 34
4.3.2.1 Grid-connected Mode 34
4.3.2.2 Isolated Mode 36
4.3.3 Change in Solar Irradiance 37
4.3.3.1 Grid-Connected Mode 37
4.3.3.2 Isolated Mode 37
4.3.4 Microgrid Isolation from the Utility 39
4.3.4.1 Microgrid Isolation Scenario 1 39
4.3.4.2 Microgrid Isolation Scenario 2 40
4.3.4.3 Microgrid Isolation Scenario 3 42
4.3.5 Microgrid Reconnection to the Utility 43
4.3.5.1 Microgrid Reconnection Scenario 1 43
4.3.5.2 Microgrid Reconnection Scenario 2 44
4.3.6 BESS SOC Limits 45
4.4 Discussion 46

Chapter 5 Conclusions and Future Work 49
5.1 Conclusions 49
5.2 Future Work 50
References 51

List of Figures

Figure 1.1: Thesis objectives 3
Figure 2.1: Two-wire DC distribution system configuration 5
Figure 2.2: Three-wire DC distribution system configuration 6
Figure 2.3: Ring-shaped DC distribution system configuration 6
Figure 2.4: Three-level hierarchical control of a DC microgrid 8
Figure 2.5: Four-operating-mode autonomous control strategy 10
Figure 2.6: Five-operating-mode autonomous control strategy 10
Figure 3.1: One-line diagram of the CERTS microgrid test bed 21
Figure 3.2: BESS electrical model 23
Figure 3.3: PV array model 24
Figure 3.4: Overall DC microgrid layout based on CERTS AC Microgrid 26
Figure 4.1: DC voltage control 28
Figure 4.2: Grid-side VSC control 29
Figure 4.3: BESS converter droop characteristics 30
Figure 4.4: BESS converter control 31
Figure 4.5: PV sources converters droop characteristics 31
Figure 4.6: PV source converter adaptive droop 32
Figure 4.7: PV source converter control 32
Figure 4.8: Simulation results of case 4.3.1 34
Figure 4.9: Simulation results of case 4.3.2.1 35
Figure 4.10: Simulation results of case 4.3.2.2 36
Figure 4.11: Simulation results of cases 4.3.3.1 and 4.3.3.2 38
Figure 4.12: Simulation results of case 4.3.4.1 40
Figure 4.13: Simulation results of case 4.3.4.2 41
Figure 4.14: Simulation results of case 4.3.4.3 42
Figure 4.15: Simulation results of case 4.3.5.1 43
Figure 4.16: Simulation results of case 4.3.5.2 44
Figure 4.17: Simulation results of case 4.3.6 45

List of Tables

Table 3.1: Cable-sizing results 22
Table 3.2: BESS model parameters 23
Table 4.1: System voltages for normal operation 33
Table 4.2: Case 4.3.2.1 system voltages 35
Table 4.3: Case 4.3.2.2 system voltages 37
Table 4.4: System volages for case 4.3.3.2 38
Table 4.5: System voltages for case 4.3.4.1 39
Table 4.6: System voltages for case 4.3.4.2 41
Table 4.7: System voltages for case 4.3.4.3 42

Chapter 1

Introduction

1.1 Motivation

Microgrids are power system entities that consist of at least one distributed generation (DG) resource [1] and that can become isolated from the main power system grid and operate as an independent island. The concept has come to the forefront with the increased utilization of DG resources such as solar, wind, fuel cells, and combined heat and power generators [2]. With proper sizing and design, these resources can operate independently from the main electrical grid to supply the local load either continuously or on an intermittent basis. Microgrids can also perform intentional islanding without affecting grid integrity in order to improve local system reliability in the case of disturbances in the main grid [3].

The increase in DG utilization can be attributed to the need for expanded generation capacity. Considering the financial issues involved, along with the right-of-way problems associated with the generation and transmission of electrical energy, DG resources can be viewed as an alternative for erecting new conventional power plants as a means of supplying power deficits [4]. With the advancements in the reliability and controllability of DG resources, the need for managing and coordinating a variety of resources and their associated loads has led to the microgrid concept. The most promising DG technologies for microgrid applications are micro-turbines, photovoltaic, fuel cells, and gas internal combustion engines with permanent magnet generators [3].

The advantages of microgrids in general are increased energy efficiency through decreased energy transmission and operational costs, a reduced carbon footprint through the integration of renewable energy resources, and improvements in power quality and availability to end users through advanced control techniques. However, several challenges are related to the realization of microgrid concept: the control of a large number of distributed energy resources [2], islanding, and energy conversion and management costs [4].

Compared to its AC counterpart, a DC microgrid has the potential to provide additional advantages that can improve power system performance: the facilitation of the interconnection of distributed energy resources and energy storage systems, and the isolation of power system disturbances from the power island [5]. However there are challenges inherited from DC systems such as synchronization and power system protection designated by fault detection and isolation.

AC microgrids were introduced first because existing electrical grids are primarily AC systems. A small portion of an existing AC grid, such as a residential community, can be converted to an AC microgrid through the installation of sufficient DG along with an isolating switch at the grid interface for islanding purposes. A DC microgrid is more suitable for new area development installations in rural areas, commercial facilities, or residential buildings [6]. However, the DC microgrid concept can also be applied for existing installations since existing AC systems are principally three-phase systems having at least three wires, which is the number of wires needed for a DC system: positive, negative, and ground [5]. Nevertheless, converting an existing system to a DC microgrid would require a considerable amount of equipment retrofitting as well as power electronic converters installations.

One of the main factors in a decision to use AC or DC microgrids is the number of converters required in the system, which is dependent on the type of DG used and the system loads connected. For example, the number of converters in a DC microgrid will be less than in an AC microgrid for a network based on photovoltaic or wind renewable energy resources. Supplying motors with variable speed drives, LED lighting, DC loads, and UPS systems from AC systems also requires multiple conversions that result in energy losses [7].

Compared to an AC system, in which frequency, phase, and reactive power control is required, a DC microgrid requires only the balancing of the active power in the system for proper voltage regulation to be ensured [6]. Due to the presence of the AC/DC converter, a DC microgrid also does not increase the short circuit capacity of the main grid at the interconnection point, and the interconnection converter can be used to mitigate power quality problems such as voltage sags, harmonics, and voltage fluctuation. All of these features result in a high-quality network [5]. In addition, DC capacitance prevents the propagation of power system disturbances between the microgrid and the main grid.

The objectives of this thesis are:

- Develop a simulation model for low voltage DC microgrid with photovoltaic distributed generation using PSCAD/EMTDC simulation environment.
- Implement power control strategy for modeled DC microgrid to ensure acceptable levels of voltage regulation and seamless transitions between grid-connected and isolated modes of operation.
- Verify the functionality of the power control strategy during different microgrid modes of operation and a variety of system perturbations such as modes transitions, and sudden changes in generation and loading conditions.

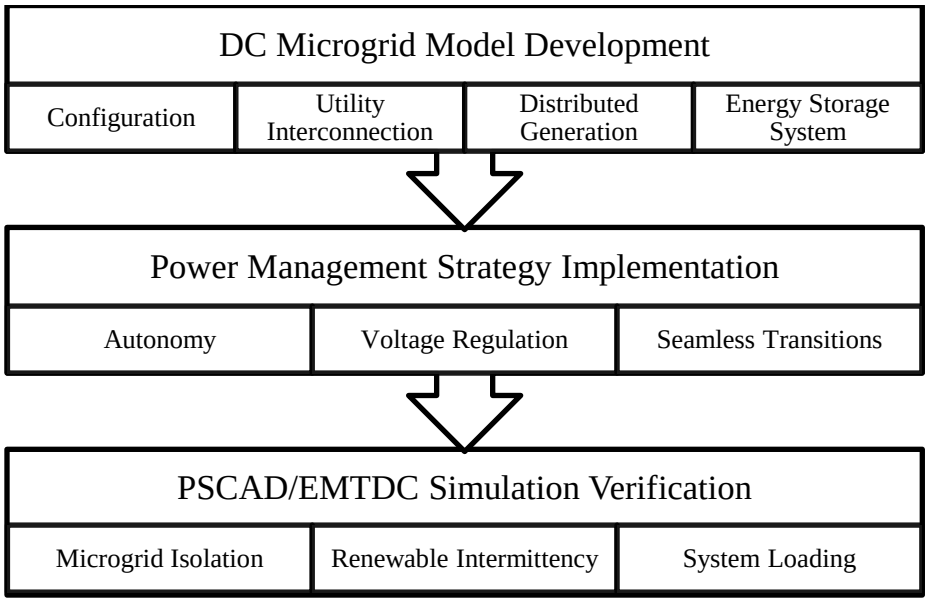

Figure 1.1: Thesis objectives

1.2 Organization of Thesis

A review of the literature related to the thesis topics is presented in Chapter 2. The review covers strategies used for controlling DC microgrids, including ones based on hierarchical control, distributed control, and intelligent control. DC distribution system configurations are then discussed, and solar energy sources and energy storage systems are reviewed from the perspective of their application for a DC microgrid.

Chapter 3 describes the modeling of a DC microgrid in PSCAD/EMTDC environment. The chapter begins with an overview of the CERTS Microgrid Test Bed, which is used as the topology for modeling a DC microgrid. The sizing of fundamental power system components is then explained, including loads, distributed generation, and feeders, followed by an introduction to the energy storage system and solar energy source models.

Chapter 4 discusses the power management strategy applied for developed DC microgrid model. The objectives of the control strategy are first outlined. Control is provided jointly through the local control of converters, including a grid-interfacing converter, a solar energy source converter, and an energy storage system converter. The control functions performed by each converter in order to implement the overall system strategy are explained. The final sections of the chapter present the simulation results of case studies conducted using the developed DC microgrid model in conjunction with the implementation of the control strategy.

Chapter 5 outlines the conclusions to be drawn from this work and suggests directions for future work.

Chapter 2

Literature Review

2.1 DC Distribution System Configurations

The literature includes references to three configurations for DC distribution systems: two-wire, three-wire, and ring-shaped. The two-wire version shown in Figure 2.1 is the most common configuration. In a two-wire configuration, cables should be designed to withstand higher voltages and greater currents than in a three-wire configuration. However, a two-wire configuration offers the advantages of lower line losses and the savings associated with fewer wires [8].

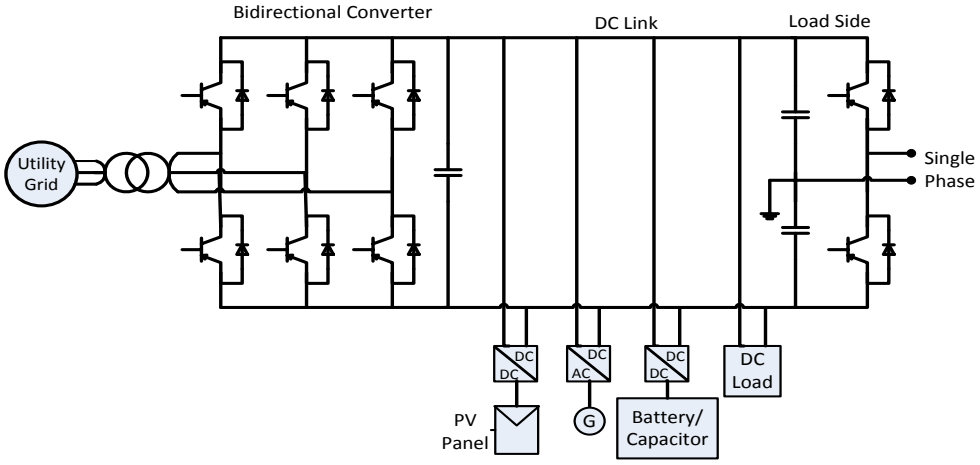

Figure 2.1: Two-wire DC distribution system configuration [8]

A three-wire configuration (Figure 2.2) is also called a bipolar-type DC system. The voltages of the three wires are $+V_{dc}$, 0, and $-V_{dc}$. This type of configuration requires a voltage balancer for balancing the positive and negative voltages located at the DC side of the AC/DC bidirectional converter. The ring-shaped configuration shown in Figure 2.3 is used to provide redundancy with respect to the power supply [9].

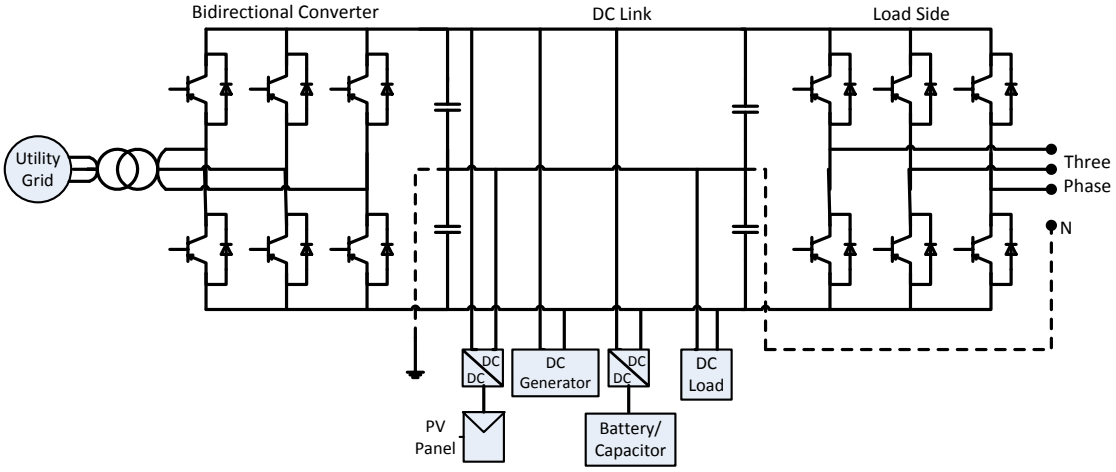

Figure 2.2: Three-wire DC distribution system configuration [8]

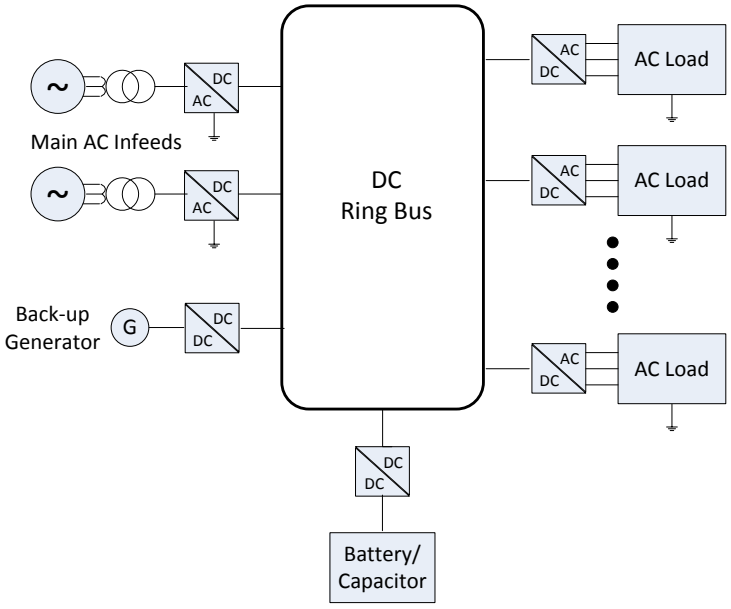

Figure 2.3: Ring-shaped DC distribution system configuration [9]

2.2 DC Microgrid Control Strategies

A DC microgrid consists of power sources, loads, and grid-interfacing converters connected in parallel to a DC bus system. Due to the line resistances of the wires connecting these elements, differing voltage levels are present at different converters and load terminals. To maintain voltages at all terminals within an acceptable range from nominal value, a balance should be maintained between the generated and consumed power levels [10]. A power management strategy is therefore needed in order to ensure voltage regulation and the stable operation of the microgrid.

The conventional method of controlling power sharing between paralleled converters is to use a central controller [10], but this technique requires communication between all system elements and the central controller, which entails additional cost and could affect system performance in the case of a communication delay or failure. Reliance on a central controller also jeopardizes the reliability of the system because the controller represents a single point of failure, and system expandability is negatively affected since the introduction of any additional element increases the complexity of the controller [6].

The literature includes reports of several proposed DC microgrid control strategies, which can be categorized as one of three primary control schemes: hierarchical control, distributed control, or intelligent control.

2.2.1 Hierarchical Control

Hierarchical control distributes system control objectives to a number of control levels. This control scheme contributes to system flexibility and expandability however it requires communication between different control levels. This scheme is also effective for a variety of system operating modes: grid-connected mode, isolated mode, load-shedding mode, and generation curtailment mode [10].

In a three-level hierarchical control strategy, the primary control level is assumed by the power sources and load converters, which control DC system voltages based on a droop control method. The secondary control level is provided by a central controller that monitors the electrical limits of the system. The tertiary level is handled by the energy management

system, which controls power flows within the microgrid and any power exchange with the main grid [10].

In the three-level hierarchical control strategy for a DC microgrid proposed in [11], the primary level controls the virtual output impedance of the converters. The secondary level controls voltage regulation in the microgrid, and the tertiary level controls the current flow between the microgrid and the main grid. Based on the three-level hierarchical control proposed in [11], a hierarchical control technique is also presented in [7], in which the tertiary level prepares dispatch schedules for power sources and storage systems. Based on the values set by the tertiary level, the secondary level controls the output power levels of the power sources and storage systems by specifying controller droop parameters. Then the primary level executes the droop control scheme based on the parameters set by the secondary level. The functioning of this strategy is illustrated in Figure 2.4.

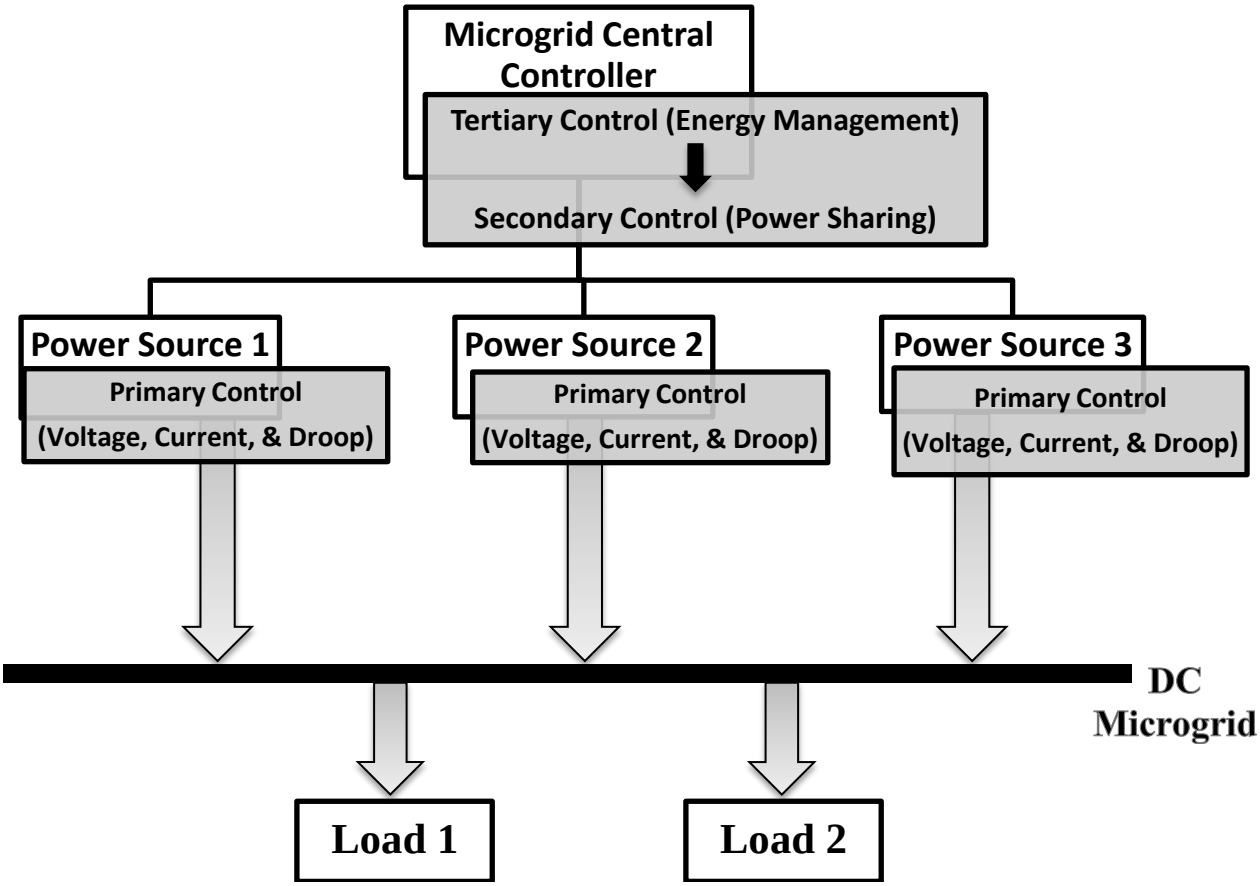

Figure 2.4: Three-level hierarchical control of a DC microgrid [7]

2.2.2 Distributed Control

In distributed control strategies, the operation of each system component is controlled by its converter based on locally obtained feedback signals. A communication system is therefore not required for this type of strategy, called autonomous distributed control. However, some intelligent distributed control strategies, such as multi-agent systems, employ communication between distributed controllers in order to reduce controllers' complexity.

2.2.2.1 Autonomous Distributed Control

An autonomous distributed control strategy should maintain satisfactory system operation under a variety of operating modes without communication between the distributed controllers. This feature reduces the complexity of the system, thus increasing its reliability and enhancing its expandability since the introduction of additional system components does not require changes to the parameters of the existing controllers.

A droop control scheme is widely used in autonomous control strategies for controlling the parallel operation of converters. In a DC microgrid, the droop characteristics of the converters can be employed for controlling power sharing: the output resistance of the converters can be varied using the droop constants of the converters, which act as virtual output resistances. To accommodate varying system operating conditions, each converter switches between different operating modes based on the deviation of its terminal voltage from the nominal value and its power rating limit [10].

The voltage level in a DC bus can be used as an indicator of the generation/load power balance in a DC microgrid [6] and has therefore been employed in autonomous control strategies as a signal for identifying the system operating mode. In [12], a four-operating-mode autonomous control strategy is proposed, in which the acceptable DC voltage range is divided into four levels. For each microgrid operating mode, the DC bus voltage is regulated to one of the four predefined levels, as shown in Figure 2.5. When the strategy described in this paper is applied for a multiple-bus DC system, the voltage tolerance between modes should be re-evaluated to include consideration of line voltage drops and voltage measurements accuracy which is defined by transducers precision.

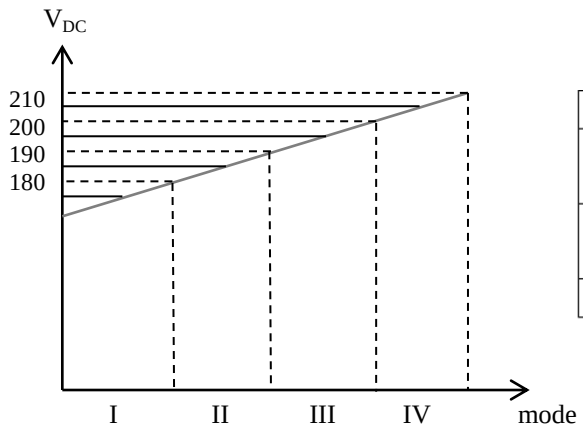

I	Isolated	Energy storage system control
II	Grid-connected	DC/AC converter control (rectification)
III	Grid-connected	DC/AC converter control (Inversion)
IV	Isolated	DG control

Figure 2.5: Four-operating-mode autonomous control strategy [12]

A five-operating-mode autonomous control strategy is proposed in [13]. The acceptable voltage range is divided into five levels that correspond to the five operating modes. Specific converters are assigned to work as slack terminals that control the DC voltage for each of the five operating modes, as shown in Figure 2.6. However, the use of an energy storage system as a slack terminal in Level 1 does not coincide with its droop characteristics for Level 2, which shows zero output power when the voltage is between A_1V_N and B_1V_N.

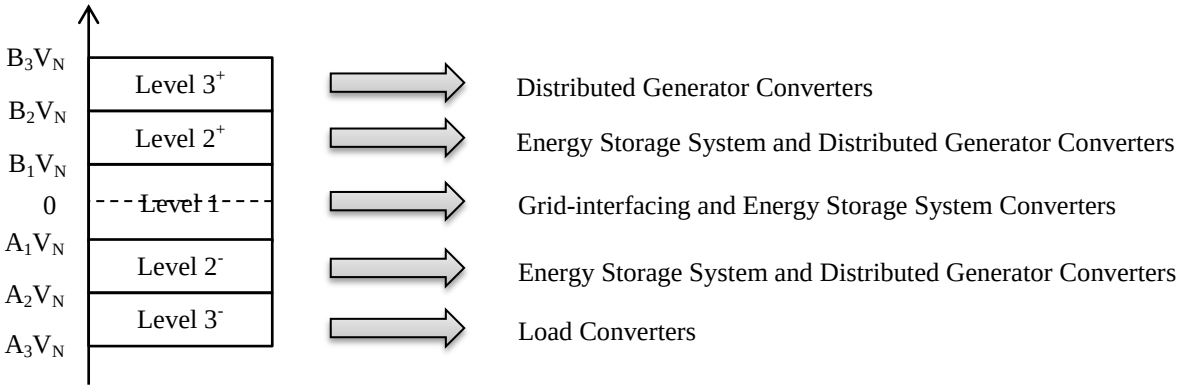

Figure 2.6: Five-operating-mode autonomous control strategy [13]

2.2.2.2 Multi-agent Control

Multi-agent control is a distributed control strategy that requires communication. This type of control system consists of several agents that have limited capabilities but that can communicate with one another to implement an overall system strategy. The use of multi-agent control has been facilitated by the emergence of fast communication devices [10].

A multi-agent system is presented in [14] for use in generation scheduling and the demand side management of a hybrid microgrid. Modeling power system components as multi-agent system entities is an effective way of representing communicating power system elements [14]. The use of a multi-agent system with a hardware-in-the-loop simulation for the implementation of emergency demand response control of a DC microgrid is described in [15]. A multi-agent system is an efficient control technique, especially for large power distribution systems [15].

2.2.3 Intelligent Control

Classical control theory can encompass unambiguous systems. However, intelligent control techniques such as fuzzy logic work better for extremely complex and uncertain systems [10]. For DC microgrid control, the literature contains reports of the use of fuzzy logic, in particular, which offers the advantage of enabling the incorporation of human best practices into controller design.

In [16], the researchers report the use of a combination of fuzzy control and gain scheduling for controlling electric double-layer capacitor storage systems: fuzzy logic control is used for balancing the energy stored in the storage systems while DC voltage control is actually carried out through scheduling the droop gains of the storage system controllers. In another study, fuzzy logic control was used for the DC voltage control of a stand-alone hybrid power plant [17]. Implementation of the fuzzy logic control proposed in this paper, however, requires a central controller that receives the voltage and current input from all distributed generators and storage systems.

2.3 Solar Energy Sources

Solar energy sources convert solar radiation to electrical power. The two types of solar sources are distinguished according to the technology utilized for energy conversion. Photovoltaic (PV) solar systems convert solar energy directly to DC electrical power when panels are irradiated by sunlight [18], while solar thermal systems convert solar energy to heat that is used to produce electricity as in conventional thermal power plants.

Solar thermal systems utilize reflectors to concentrate the solar radiation energy. The concentrated energy is focused onto heat absorbers, which could be pipes or a solar tower. The heat absorbed is then used to increase the temperature of a thermal material that transfers the heat to a water steam cycle by means of a heat exchanger. Finally, the steam cycle is used to drive a conventional steam turbine generator that produces electrical power [19].

PV solar systems can be as small as a few panels located on the roof of a residential building. However, their size and capacity have been increasing, and large PV plants consisting of numerous panels mounted on a large ground area can reach capacities comparable to those of existing thermal power plants. Concentrators can also be employed to increase the solar radiation on PV panels, thus reducing the size of the panels required for producing a specific amount of electrical power [19].

For DC microgrid applications, a PV solar system is more advantageous than a solar thermal system because it produces DC electrical power directly, while a solar thermal system utilizes conventional power generators that produce AC electrical power. Employing PV solar systems for DC microgrid applications therefore requires less power conversion in the electrical system. All of the solar distributed sources described in the literature for use with DC microgrid systems are PV-based solar sources.

In the study presented in [20], a PV source was used for distributed generation in an isolated renewable DC microgrid. The authors used maximum power-point tracking (MPPT) to maximize the power output from the PV sources. The PV source power is curtailed only in light system load conditions. This strategy was shown to be effective for utilizing available low-cost renewable energy [20].

The use of a PV source as part of an intelligent DC microgrid with smart grid communications is described in [21]. The researchers proposed a control strategy for handling the intermittency of renewable sources. The strategy includes consideration of renewable PV power as a high priority through MPPT operation in most system operating conditions. The strategy also takes into account turning off the PV source in the case of low solar irradiance where it would not be economically feasible to operate the PV source. Two modes are considered for grid operation: normal mode with no limits for grid power exchange and constrained mode with limits on the power exchanged with the grid. However, DC microgrid isolated mode of operation is not mentioned in this study [21].

2.4 Energy Storage Systems

In DC microgrid applications, energy storage systems (ESSs) are used for supplying or absorbing any power mismatch between the generation and the load. This function is particularly important for DC microgrids that are based on renewable energy resources due to the uncertainty and random nature of renewable energy sources, and it also supports the autonomous operation of microgrids because the available renewable energy can be stored and then supplied to meet the local load demand when needed. Several storage system technologies are mentioned in the literature for use with DC microgrid applications: electric double-layer capacitors, batteries, flywheels, and superconducting magnetic energy storage.

2.4.1 Electric Double-Layer Capacitors

Electric double-layer capacitors (EDLCs) are also called supercapacitors or ultracapacitors. The construction of an EDLC is similar to that of a battery, with two electrodes inserted into an electrolyte, and a dielectric separator between the two electrodes. The surface of the two electrodes has a large number of micropores, creating a large surface area where the charges build up. Energy is stored in the dielectric material as electrostatic energy [22].

Compared to battery storage, EDLCs offer faster responses, lower maintenance, and longer life cycles. However, their energy storage capability is limited, making them suitable only for short-term storage. They are typically used in power bridging for periods ranging from seconds to a few minutes, in cases when the main supply fails [8][22].

In conjunction with a battery storage system, an ELDC with a one farad capacitance is described in [23] for the provision of transient compensation. The ELDC is controlled by a bidirectional chopper in order to maintain a constant DC voltage in situations in which the reference power is determined by a central controller. Battery energy storage system was also used for DC voltage regulation by maintaining generation/load power balance. Simulation results showed how the ELDC and battery system controlled the DC voltage during transients. However, the reason for using two energy storage technologies to perform the same function is not explained.

An ELDC storage system for a residential DC microgrid with dispatchable distributed generation units is presented in [24]. It was used for controlling the DC voltage of the microgrid in isolated operation mode and also for voltage clamping in grid-connected mode when the DC voltage exceeds specified upper and lower limits. A DC microgrid with an ELDC and battery energy storage is presented in [25]. In the system described, designing storage device converters with different time constants enables the ELDC to be used for managing fast fluctuations in the DC voltage, while the battery handles slower transients.

2.4.2 Batteries

Battery energy storage systems (BESSs) are currently the dominant energy storage technology due to their high energy density, long lifetime, and low cost. Because of their economic energy density, lead-acid batteries are commonly used for constructing BESSs for microgrid applications. Valve-regulated lead-acid batteries are sealed batteries, which are more reliable than flooded lead-acid batteries since they do not require frequent maintenance [8][22][26].

The authors of [27] utilized a BESS for constant voltage control of a DC microgrid under normal operation and AC line fault condition. They used a lithium-ion battery model in

which the state of charge (SOC) is determined by integrating charging and discharging power. The use of a BESS is also reported in [28] as a means of compensating for the power mismatch that occurs between the variable generation and the loads under islanding and fault conditions. The researchers used the generic battery model presented in [29]. Lead-acid batteries are commonly used for PV-based renewable systems [21]. To deal with the uncertainty of PV generation, a battery storage system was used for the work described in [21], in which a valve-regulated lead-acid battery was included in the experimental setup employed for the validation of the control strategy.

2.4.3 Flywheels

Flywheel storage systems are based on the fact that energy can be stored in the spinning mass of a flywheel that is coupled with an electrical machine. The energy is transferred to the flywheel when the machine is operated in motor mode in order to accelerate the flywheel shaft. Energy can then be transferred back to the electrical system when the machine is operated with regenerative braking to slow down the rotation of the shaft. As energy storage devices, flywheels offer significant capacity, high efficiency, and fast operation. However, they cannot store energy for long periods, and the energy can be retrieved from the flywheels for only short durations. [8][22]

A flywheel storage system is described in [30] for use with a DC microgrid application. The flywheel system was employed for controlling the DC voltage through its ability to supply or absorb the difference in power between the generation and the load. The system presented utilizes an inexpensive squirrel-cage induction machine but requires an AC-to-DC converter to enable connection to a DC microgrid. The authors of [31] used a hybrid flywheel/battery energy storage system for a DC microgrid based on wind generation. They employed a permanent magnet synchronous machine as a flywheel and connected it to the system through a bidirectional AC-to-DC converter. A BESS is used in conjunction with the flywheel because the latter cannot regulate the DC voltage while in speed control mode: it must first be driven to a high speed before it can be switched to voltage control mode.

2.4.4 Superconducting Magnetic Energy Storage

In superconducting magnetic energy storage (SMES), energy is stored in a magnetic field created by passing current through an inductor. The inductor is fabricated using a superconducting material and is kept at a very low temperature in order to maintain its superconducting properties. Energy is transferred to the SMES storage through the application of a positive voltage across the inductor and is then transferred back to the electrical system through the application of a reverse voltage [22]. SMES storage is costly and has a low bridging time ranging from one to two minutes. However, it also offers high efficiency and fast response times and can provide grid frequency support [8][18]. The use of SMES is reported in [32] as a means of mitigating low-voltage ride-through and power fluctuation problems in wind doubly-fed induction generators connected to a DC microgrid. However, the effect of this technique on the DC bus voltage is not indicated in the simulation results.

2.5 Summary

The literature review conducted for this work included reports of investigations of a variety of control strategies and their optimization for DC microgrid application. These strategies include hierarchical, distributed, and intelligent control strategies. Using a central controller that determines reference set points for all other controllers jeopardizes system reliability because the loss of the central controller disturbs all control functions. Hierarchical control provides enhanced reliability since some system control functions can be sustained by the primary control level in cases involving the failure of the central controller, which performs only the secondary and tertiary control levels. This type of strategy can also provide additional control functions, including the management of the energy flow between the microgrid and the utility or between the microgrid and other microgrids, a feature that contributes to system flexibility and expandability.

Distributed control strategies are widely used for microgrid control. Autonomous distributed strategies, in particular, have been the subject of significant interest because they reduce the complexity of the control system, thus improving system reliability since

controllability is unaffected by communication link delays or controller failure. Autonomous control also offers an advantage that is important for microgrid systems: plug-and-play functionality, which allows the addition of distributed generation to the microgrid without major modifications to the existing control scheme.

As an intelligent control strategy, fuzzy logic has been used for the control of DC microgrid systems. The fuzzy logic algorithms that have been proposed require input from all system sources and storage devices. Some communication topology is therefore needed in addition to an intelligent processor for running the fuzzy logic algorithm.

The DC microgrid systems described in the literature are single-bus systems with all system components connected in parallel to the same bus. Multiple-bus low-voltage DC distribution systems have not been considered. Three-wire and ring-shaped DC distribution configurations provide greater reliability than a two-wire configuration. However, a two-wire configuration requires less wiring and leads to lower line losses.

PV energy sources are the most common renewable energy sources used with DC microgrids since they provide DC output power. An MPPT control algorithm is generally used for PV sources as a means of maximizing their output power. However, power derived from PV sources can be curtailed in light loading condition when the power can be neither exported nor stored due to islanding or power limits.

Energy storage systems have been considered for use in microgrid systems with respect to a variety of applications, including renewable energy reserves, voltage regulation, and power quality improvement. BESSs and EDLCs are the storage devices most commonly used for DC microgrid systems. Due to their high power density, BESSs can regulate DC voltage by maintaining the microgrid power balance through their ability to supply the power deficit or absorb extra power. EDLCs offer lower energy storage capability but faster response times than BESSs and are therefore employed to provide fast compensation for voltage fluctuations and short power bridging times. Flywheels are an additional promising storage technology for microgrid applications. However, a flywheel system requires an AC-to-DC converter in order to be integrated into a DC microgrid system.

Based on the aforementioned discussion of work presented in literature, this work will address the following issues:

- Develop a PSCAD model of a multiple bus low voltage DC microgrid using the layout and parameters of an actual microgrid test system.
- Implement one of the power control strategy presented in literature on the developed model and modify it as needed to achieve a high functionality of DC microgrid system.
- Propose a control technique to maximize the utilization of power available from renewable energy resources while ensuring acceptable levels of system voltage regulation.

Chapter 3

DC Microgrid System Model

3.1 CERTS Microgrid Test Bed Overview

The Consortium for Electric Reliability Technology Solutions (CERTS) has developed a microgrid concept in order to achieve a high level of functionality with low engineering costs. Meeting these goals involves three main objectives: develop a seamless transition between grid-connected and isolated microgrid operating modes, provide fault protection in case of low fault currents, and design microgrid control that operates without high bandwidth communication in order to ensure voltage and frequency stability in microgrid isolated mode [33].

To demonstrate the new microgrid concept, the CERTS Test Bed project was built in Columbus, Ohio. The system control design included consideration of plug-and-play functionality so that the addition of any new distributed generator does not require a redesign of the system's controls. A distributed control strategy was also used as a means of ensuring system reliability by avoiding a single point of failure. In addition, the microgrid was designed for seamless isolation from the main grid in the case of grid disturbances [33].

Figure 3.1 shows a one-line diagram of the CERTS microgrid test bed, which is based on radial distribution with three feeders, A, B, and C, operating at 480V AC. Four load banks

are distributed on the three feeders, with controllable power of 0-90 kW and 0-45 kVAR. Three combined heat and power (CHP) distributed generation (DG) units are also located at feeders A and B. The CHP units are connected to the system through 60 kW ± 60 kVAR inverters [33].

In this work, the CERTS Microgrid Test Bed system was used as the topology for modeling a DC microgrid with respect to feeders, loads, and DG. However, a bidirectional AC/DC converter was included at the secondary side of the grid interfacing transformer, and some loads were considered to be DC loads. As well, two of the DG units were considered to be PV sources, while the third was replaced by an energy storage system.

3.2 Power System Component Sizing

This section details the sizing of the power system components including the loads, DG, and feeders. The DC voltage used for sizing was 1000V DC, which is the selected nominal DC voltage of the microgrid, as explained in the next chapter.

3.2.1 Loads

The four load banks were modeled as two variable 60 Hz three-phase AC loads and two variable DC loads. The DC loads were sized from 0 kW to 90 kW and were modeled as variable resistance while AC loads were sized at 90 kW, 45 kVAR, and modeled using a constant PQ load model. The AC loads were rated at 480 V and were connected to the DC microgrid through three-phase voltage source inverters. Voltage control was implemented for the inverters using a sinusoidal pulse width modulation (SPWM) control technique. The low-pass filter used to smooth the output of the inverter was sized for the maximum reactive power of the connected load.

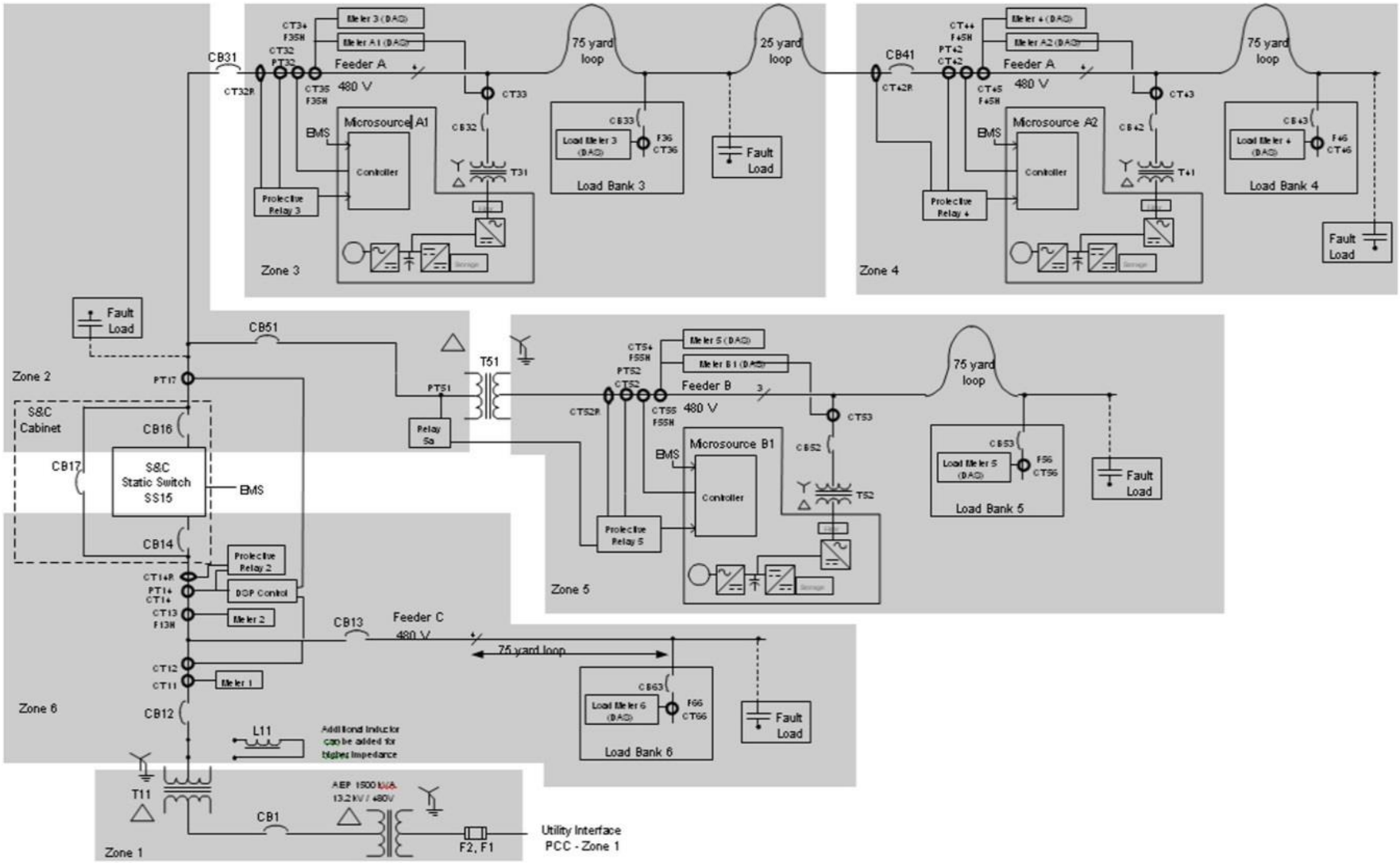

Figure 3.1: One-line diagram of the CERTS microgrid test bed [33]

3.2.2 Feeders

The feeders were modeled according to their resistance, and their sizes were determined based on the ampacity required for handling the maximum load and generation at the rated DC voltage. The DC resistance of the cables was then calculated based on consideration of their lengths as specified in the one-line diagram of the CERTS microgrid. Table 3.1 summarizes the cable-sizing results.

Table 3.1: Cable-sizing results

Zone	Feeder	Length (yard)	Ampacity (Amps)	Size (AWG)	Resistance (mΩ)
Zone 3	A	75	180	4/0	14
Zone 3	A	25	160	4/0	4.67
Zone 4	A	75	90	1	36
Zone 5	B	75	90	1	36
Zone 6	C	75	90	1	36

3.3 Energy Storage System Model

Based on the literature review, a battery energy storage system (BESS) was selected because it is the technology most suitable for a DC microgrid with renewable energy resources. The model used for the BESS was a valve-regulated lead-acid battery model since it is the battery type most commonly employed in microgrid applications. The nonlinear electrical model presented in [34] was modeled in PSCAD without consideration of the battery voltage relaxation effect. The BESS was then integrated into the DC microgrid system through a bidirectional buck-boost converter.

The modeled circuit is shown in Figure 3.2, in which the left-hand part illustrates the integration of the charging and discharging current in order to determine the state of charge (SOC) of the BESS. The capacitance represents the BESS capacity, while the voltage across the capacitance represents the SOC. The components shown in the right-hand part of the figure represent the dynamic performance of the BESS; their values were obtained using the equations detailed in Table 3.2.

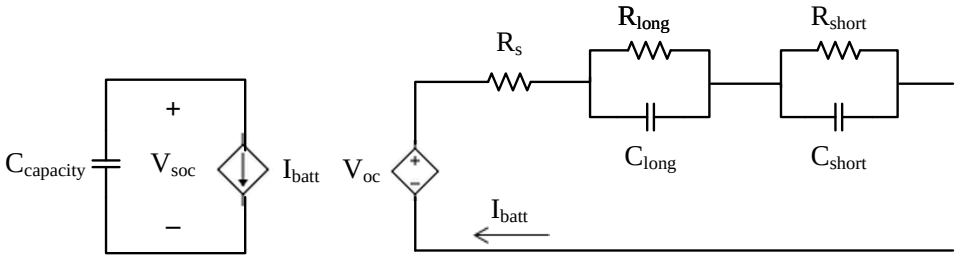

Figure 3.2: BESS electrical model [34]

Table 3.2: BESS model parameters [34]

During BESS Charging	During BESS Discharging
$V_{oc} = 1.963 + 0.334 * V_{soc} - 0.113\, SOC^2$	$V_{oc} = 1.946 + 0.242 * V_{soc} - 0.0218\, {V_{soc}}^2$
$R_s = 0.000625 + 0.000147 * V_{soc}$	$R_s = 0.000729 + 0.00164 * e^{-15.95 * V_{soc}}$
$C_{long} = 302000 + 54400 * e^{5.962 * V_{soc} - 0.251}$	$C_{long} = -3594000 + 8810000 * e^{1.068 * (0.8 - V_{soc})}$
$C_{short} = 7960 + 12870 * V_{soc}$	$C_{short} = 8710 + 2080 * V_{soc} + 10000 * (1.5 * V_{soc} - 1.135)^2$
$R_{long} = 0.000516 + 0.0049 * e^{21.65 * V_{soc} - 16.565}$	$R_{long} = 0.000142 + 0.0167 * e^{-170.3 * V_{soc}}$
$R_{short} = -0.000946 + 0.00228 * e^{-4.15 * V_{soc}} + 0.00502 * V_{soc}$	$R_{short} = -0.00398 + 0.00467 * e^{-1.15 * V_{soc}} + 0.00379 * SOC$

3.4 Solar Source Model

PV energy sources were used as the DG units in the DC microgrid model. The PV array model in the PSCAD components library was integrated into the DC microgrid system through a boost converter. The model is based on the dynamic PV array model presented in [35]. The PV array equivalent circuit is shown in Figure 3.3, and the relationships between the circuit currents are given by equations (3.1)-(3.4) [36]:

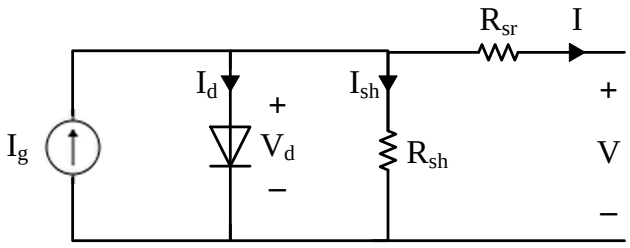

Figure 3.3: PV array model [36]

$$I = I_g - I_d - I_{sh} \tag{3.1}$$

$$I_g = I_{ScR} * \frac{G}{G_R}\left[1+\alpha_T(T_c - T_{cR})\right] \tag{3.2}$$

$$I_d = I_o * e^{\left(\frac{V+I*R_{sr}}{nkT_c/q}\right)} - 1 \tag{3.3}$$

$$I_o = I_{oR} * \left(\frac{T_c}{T_{cR}}\right)^3 * e^{\left[\left(\frac{1}{T_{cR}} - \frac{1}{T_c}\right)*\frac{qe_g}{nk}\right]} \tag{3.4}$$

where I_{ScR}: Short-circuit current

G_R: Reference solar radiation

T_{cR}: Reference cell temperature

α_T: Temperature coefficient of the photo current (α_T = 0.00017 for Silicon cells)

I_o: Saturation current

q: Electron charge

e_g: Solar cell band-gap energy

n: Diode ideality factor (typically, n = 1.3 for silicon solar cells)

k: Boltzmann constant

3.5 Summary

A low-voltage DC microgrid model with PV distributed generation has been developed using PSCAD/EMTDC simulation environment. The developed DC microgrid model is based on the CERTS AC microgrid system, which is the best-known microgrid system reported in the literature and includes readily available parameters. However, for this work, modifications were necessary in order to convert it to a DC microgrid system, including the addition of a bidirectional AC-DC converter at the point of interconnection with the utility. Two DG units were also modeled as PV energy sources, while the third DG unit was modeled as an energy storage system, as required for the power management strategy described in the next chapter. In addition, two of the four loads were modeled as DC loads. The final layout of the modeled DC microgrid system is as shown in Figure 3.4. The BESS and PV source-2 are connected at the beginning of feeders A and B respectively.

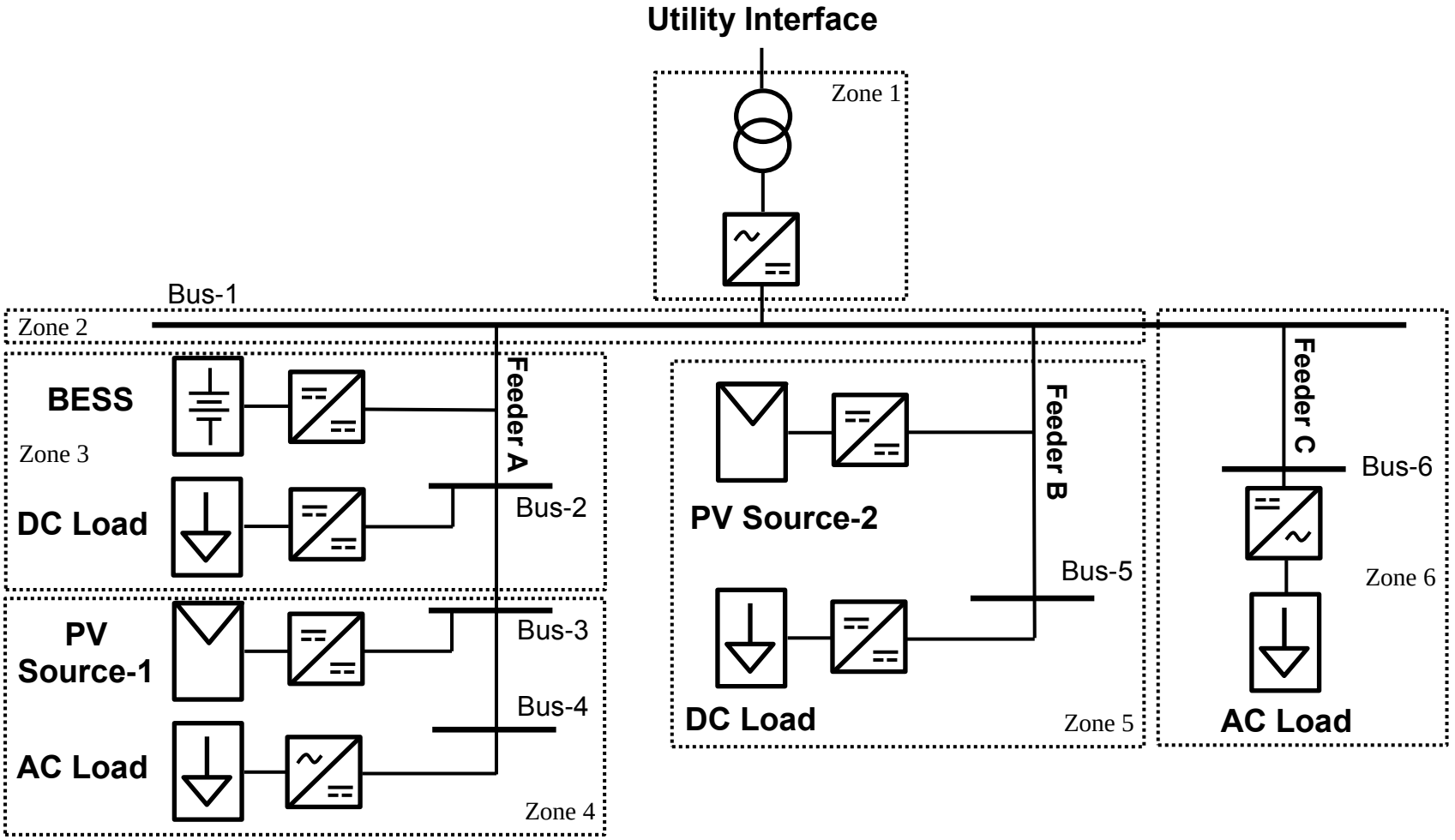

Figure 3.4: Overall DC microgrid layout based on CERTS AC Microgrid

Chapter 4

Power Management Strategy

4.1 Control Strategy Objectives

The primary objective of the power management strategy for the DC microgrid is to ensure DC voltage regulation within an acceptable range for all DC distribution buses. As is evident from the literature review, several control techniques can achieve this objective. However, for this work, an autonomous distributed control strategy is desirable for several reasons. First, autonomous control does not rely on communication links that could affect system reliability in the case of delays or failures, and it is also not dependent on a central or master controller that constitutes a single point of failure. In addition to providing control system reliability, the absence of a central controller and communication topology also reduces installation and operating costs. Another advantage of autonomous control is that it enhances the plug-and-play functionality of the microgrid since the addition of components does not entail modifications to the existing system control or communication topology.

Another important objective of the DC microgrid control strategy is to ensure a seamless transition between grid-connected and isolated modes: the effects on the microgrid loads should be minimized in cases involving intentional or emergency disconnection from the main grid. Another control objective considered for this work is the maximization of the use of renewable energy, which is achieved by supplying the maximum available power from renewable sources and avoiding power curtailment unless it is necessary to satisfy a more important objective.

4.2 Implemented Control Strategy

The control strategy implemented in this work is based on the five operating modes autonomous control strategy proposed in [11]. However, adaptive droop control for distributed generation (DG) controllers was proposed in order to maximize renewable power utilization while ensuring DC voltage regulation. In each of the five operating modes, DC voltage regulation is maintained by specific controllers, either through constant voltage control or voltage droop control, as shown in Figure 4.1. The DC voltage tolerance used for this work is a deviation of ±5% from the nominal voltage for grid-connected mode and ±10 % from the nominal voltage for isolated mode.

In this control strategy, the DC voltage level is used as a signal for identifying the operating mode of the system. Each converter in the system thus assumes a specific control mode based on the deviation of its terminal voltage from the nominal value. Feeders voltage drop was not accounted for in this work since the low voltage system does not consist of long feeders. The control modes related to the grid-side, DG, and ESS converters are explained in the following sections. However, load-shedding control was not implemented in this work.

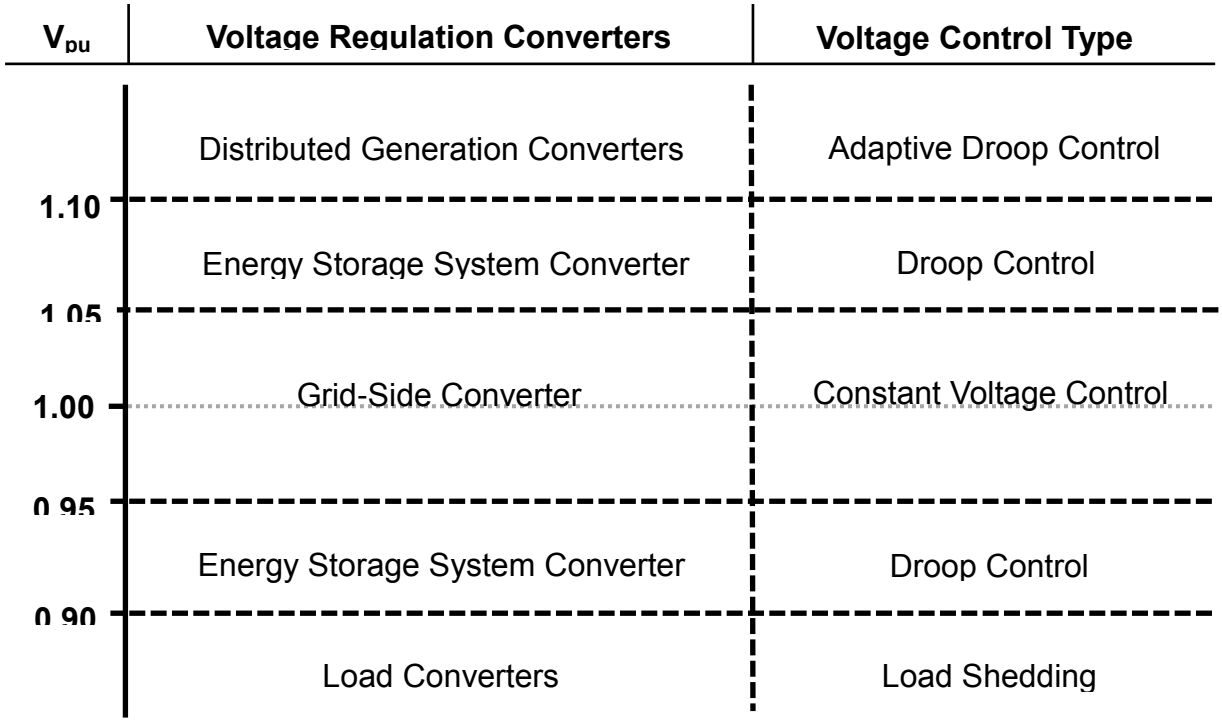

Figure 4.1: DC voltage control

4.2.1 Grid-Side Converter Control

A grid-side converter is a bidirectional, three-phase AC/DC voltage source converter (VSC). It can supply power in both directions: from the utility to the microgrid in rectification mode, and from the microgrid to the utility in inversion mode. The VSC is controlled using a sinusoidal pulse width modulation (SPWM) technique through a decoupled vector control in a dq-frame, which is a type of current-mode control. In a dq frame, the active and reactive power exchanged between the VSC and the utility are proportional to the d-axis and q-axis currents, respectively. This effect is achieved by setting the q-axis voltage to zero using a phase-lock loop (PLL) circuit that determines the angle θ for the abc-dq transformation. A block diagram of the grid-side VSC control is shown in Figure 4.2 [37], and the relationships between the VSC power and the dq-frame variables are given by the following expressions:

$$P = \frac{3}{2}\left(V_d I_d + V_q I_q\right) \tag{4.1}$$

$$Q = \frac{3}{2}\left(-V_d I_q + V_q I_d\right) \tag{4.2}$$

As shown in Figure 4.1, the grid-side VSC control was designed to provide constant voltage control of the DC bus voltage. It should maintain a 1.0 per-unit DC voltage at the grid-VSC terminal, and as a result, all other system voltages will be within ±5% of the nominal value. However, when the DC voltage at the energy storage system (ESS) converter terminal exceeds a ±5% deviation from the nominal value, BESS controller will switch to droop control mode, assuming that the grid-VSC is no longer regulating the DC voltage.

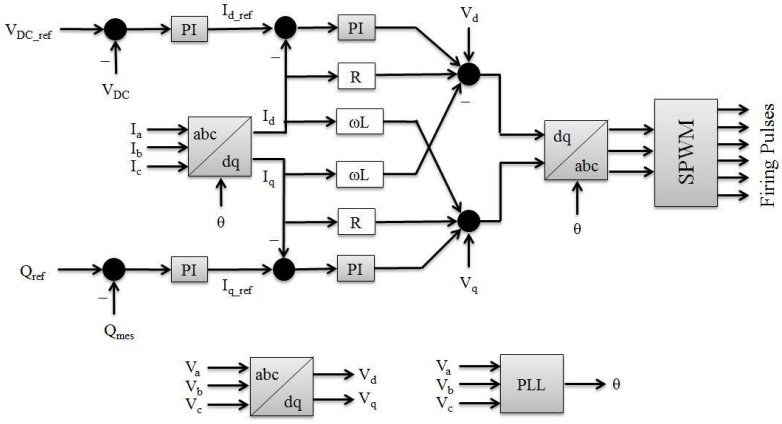

Figure 4.2: Grid-side VSC control

An important consideration related to the grid-side VSC is the selection of the DC bus voltage level. For effective operation of the VSC, the relationship between the AC and the DC voltage should satisfy the following inequality, where $\hat{V}_t$ is the amplitude of the AC phase voltage [37]:

$$V_{DC} \geq 2\hat{V}_t \tag{4.3}$$

In this work, the AC phase voltage of the utility is 277.13 V, with an amplitude of 391.92 V. Based on the above inequality, the minimum DC bus voltage is 783.84 V. To allow a DC voltage tolerance range, 1000 V was selected as the nominal DC voltage.

4.2.2 ESS Converter Control

A BESS converter is a bidirectional buck-boost converter. The control of the converter was designed for droop voltage control of the DC bus when the voltage level exceeds a ±5 % deviation from the nominal value, as shown in Figure 4.3. However, the BESS will reach its maximum charging/discharging rate when the voltage level reaches a deviation of ±10 % from the nominal value so that it no longer controls the DC voltage. As well, as long as the voltage level is within ±5 % of the nominal value, the BESS will be in standby mode, assuming that the system is grid-connected and that the grid-VSC is controlling the voltage. BESS converter control is illustrated in Figure 4.4 where V_{mes} is the measured voltage at BESS converter terminals and V_{zp} is the reference voltage at zero power.

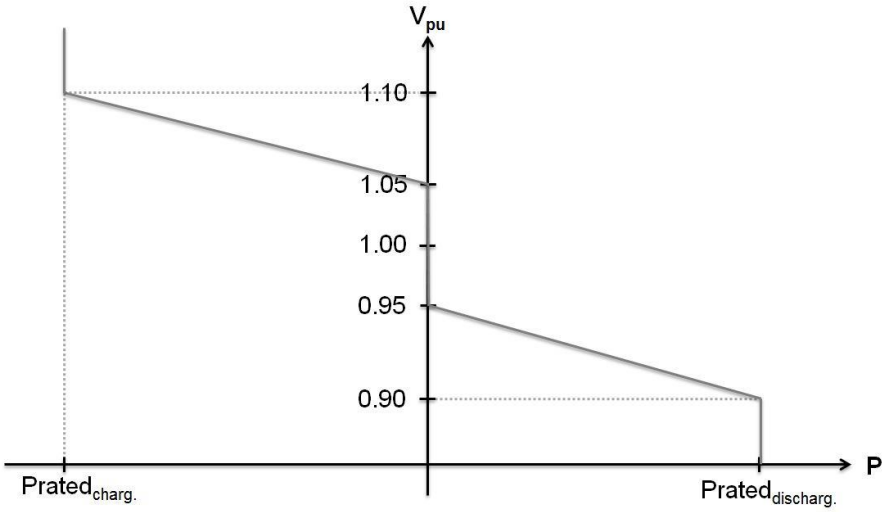

Figure 4.3: BESS converter droop characteristics

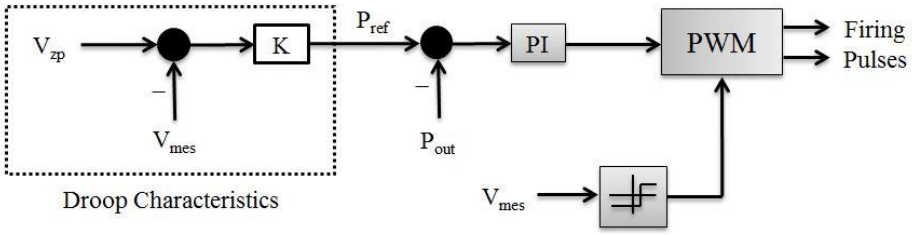

Figure 4.4: BESS converter control

4.2.3 DG Converter Control

The two PV energy source converters are boost converters, both of which are normally controlled by means of a maximum power-point tracking (MPPT) control algorithm in order to maximize the power supplied from the PV sources. However, when the voltage level exceeds the voltage tolerance limit of a +10 % deviation from the nominal value, adaptive droop voltage control is used.

Figure 4.6 shows the droop characteristics of the PV sources converters. The slope of the curve represents the droop constant, and as can be seen in the figure, the slope is proportional to the rated power of the PV source. Having droop constants proportional to rated power allows proportional power sharing between the two PV sources.

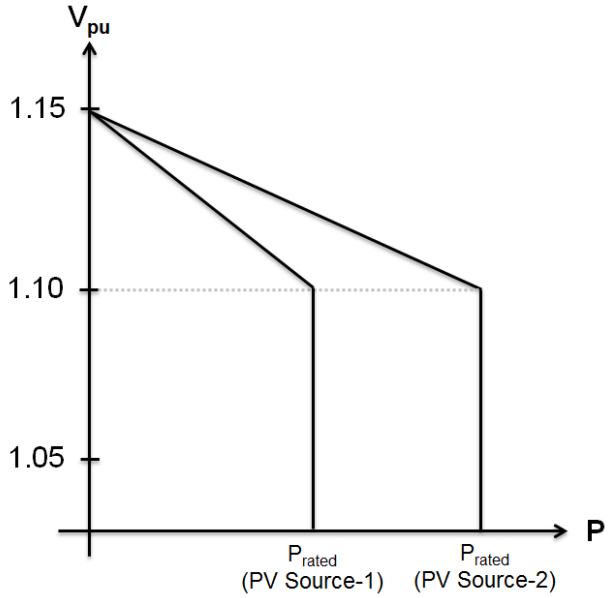

Figure 4.5: PV sources converters droop characteristics

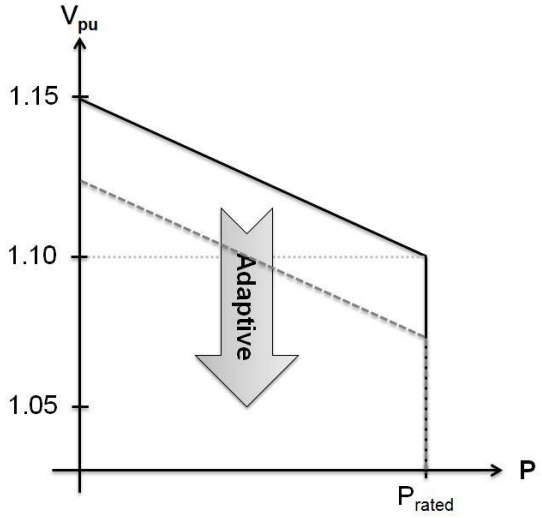

Figure 4.6: PV source converter adaptive droop

As indicated in Figure 4.6, the droop characteristic is adaptive. When the voltage exceeds a 1.1 per-unit level, the converter starts drooping the PV output power in order to limit the increase in system voltage. At the same time, it shifts the droop characteristic down in order to bring the voltage at the PV terminal to less than the 1.1 per-unit level. Once both objectives are achieved, the droop characteristic is fixed until the next time the DC voltage exceeds the limit. Using adaptive rather than fixed droop characteristics enhances the renewable power utilization since the PV source can continue working in MPPT mode until the voltage tolerance limit is violated. This advantage is due to the ability of the adaptive droop to restore the voltage to an acceptable range, a benefit that cannot be achieved with fixed droop characteristics. The PV source converter control is illustrated in Figure 4.7.

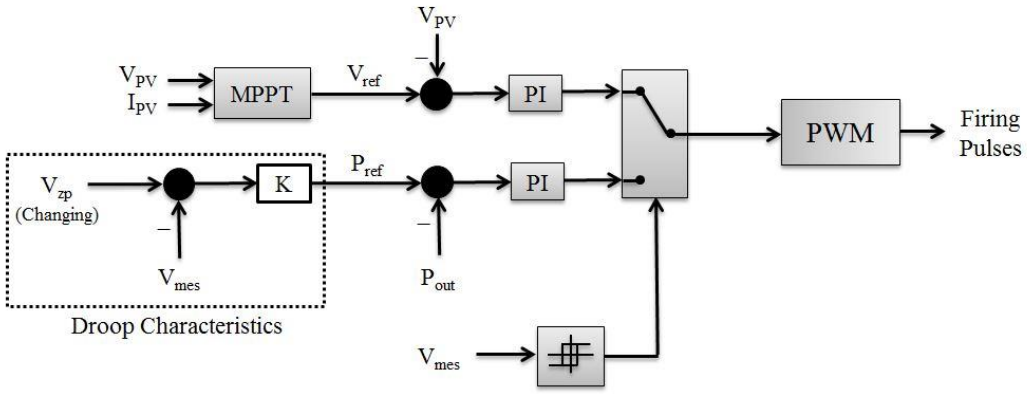

Figure 4.7: PV source converter control

4.3 Simulation Results

Simulation case studies were carried out using PSCAD power system simulator as a means of demonstrating the DC microgrid operation and control strategy. Case studies included normal system operation at maximum loading conditions, system performance during step changes in the loading or generation, and microgrid isolation from and reconnection to the utility under a variety of operating conditions. The simulation time step used for these cases was 10 μs. The output measured was smoothed using a real pole function to simulate transducer delays. The following discussion does not include consideration of system transients because the focus is on steady-state control.

4.3.1 Normal System Operation

For the first case, case 4.3.1, the system is in normal operating mode and is connected to the utility grid with the grid-VSC controlling its terminal DC voltage so that it is kept at a 1.0 per-unit level. The two PV sources are assumed to be operating at rated power levels of 160 kW and 200 kW with MPPT control. The BESS is in standby mode, and the loads are at a maximum level of 90 kW for DC loads and 90 kW, 45 kVAR, for the AC loads. Table 4.1 lists the voltages for normal operating mode. Figure 4.8 shows the simulation results for this case. Since the total load is equal to the total generation in this case, the power exchange with the utility is minimal representing system losses.

Table 4.1: System voltages for normal operation

Bus Number	1	2	3	4	5	6
Voltage (p.u.)	0.999	0.999	0.999	0.997	0.996	0.996

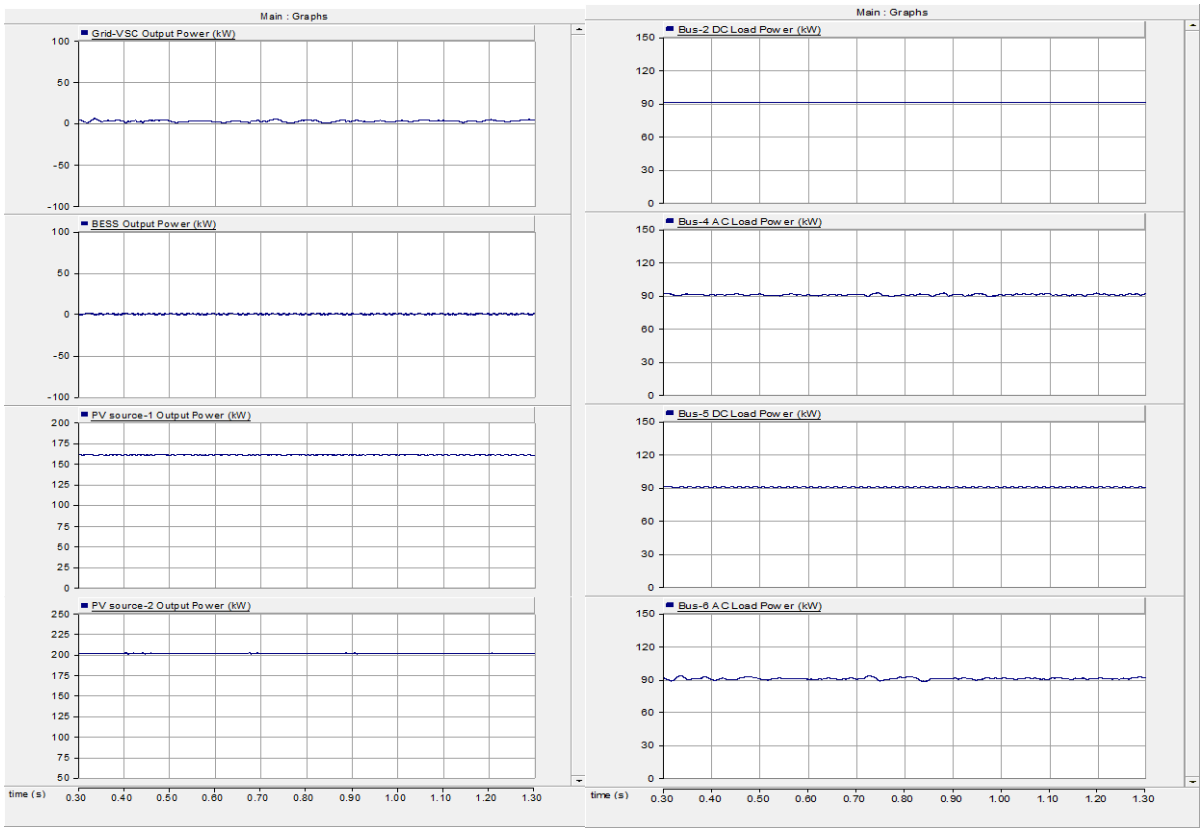

Figure 4.8: Simulation results of case 4.3.1

4.3.2 Step Load Changes

The following case studies demonstrate the system performance during step load changes in both grid-connected and isolated modes.

4.3.2.1 Grid-connected Mode

Figure 4.9 shows the simulation results for case 4.3.2.1. For this case, the bus-4 load was reduced from 90 kW to 45 kW at t = 0.5 sec. It can be seen that after t = 0.5 sec, the grid-VSC begins to export about 45 kW, which represents the excess generation resulting from the load reduction. Small changes in system voltages are also evident, as shown for bus-4, which changes from a 0.997 to a 1.0 per-unit level. Table 4.2 shows the system voltages before and after the change in the bus-4 load.

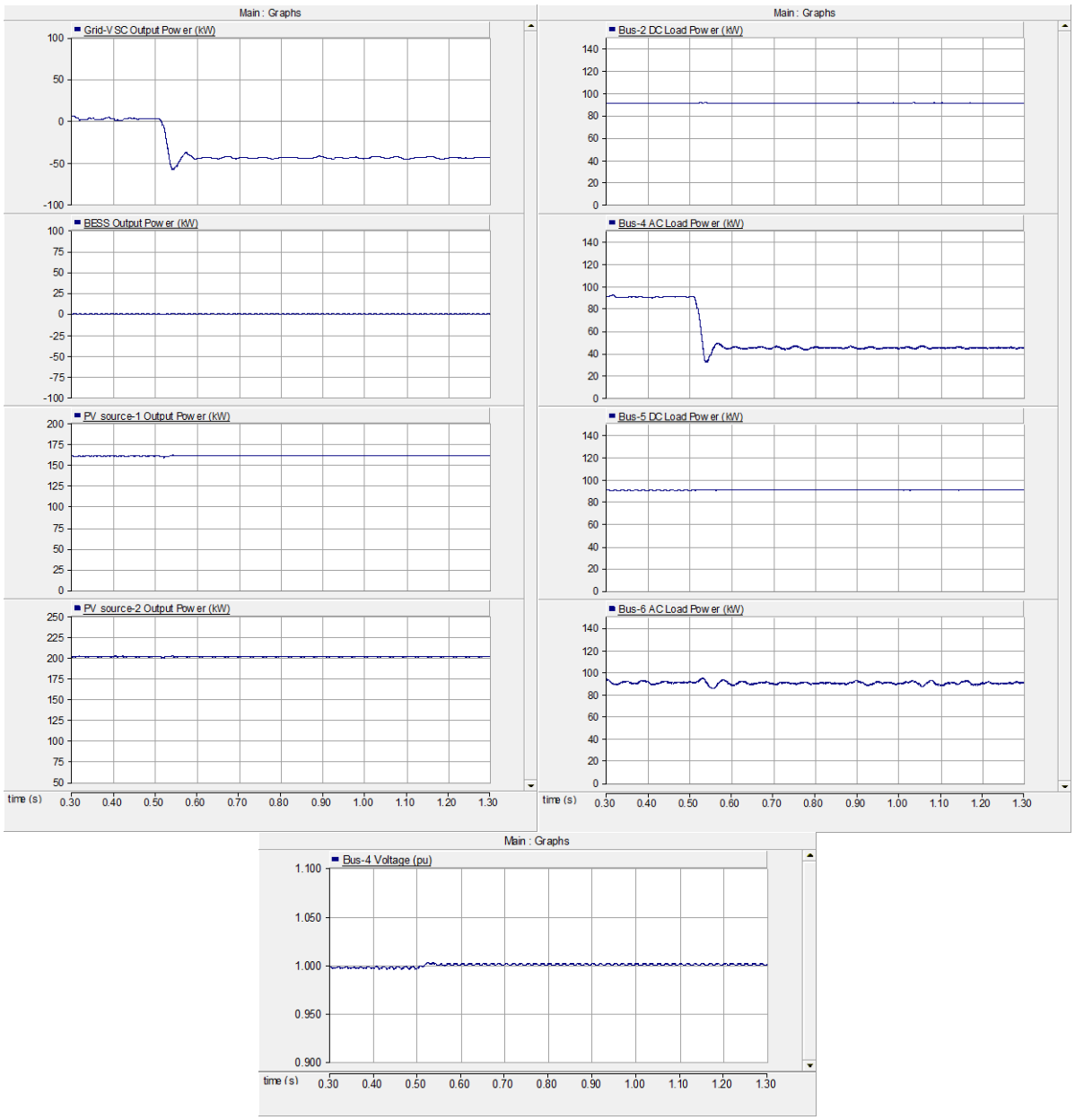

Figure 4.9: Simulation results of case 4.3.2.1

Table 4.2: Case 4.3.2.1 system voltages

Bus Number	1	2	3	4	5	6
Before	0.999	1.000	1.001	0.997	0.997	0.996
After	1.000	1.001	1.002	1.000	1.998	0.997

4.3.2.2 Isolated Mode

As shown in Figure 4.10, in case 4.3.2.2, the bus-4 load was reduced from 90 kW to 45 kW at t = 1.0 sec. In microgrid isolated mode, the BESS regulates the DC voltage so that after t = 1.0 sec, the charging power of the BESS increases from 62 kW to 108 kW, which represents the excess generation resulting from the reduction in the load. Table 4.3 shows the system voltages before and after the change in the bus-4 load. PV sources are operating higher than their rated output power because their terminal voltages are higher than rated voltage. After the step load change, there is a small increase in PV sources output power as a result of increase of their terminals voltage which attributes to the difference between the increase of BESS power (46 kW) and the 45 kW reduction in load.

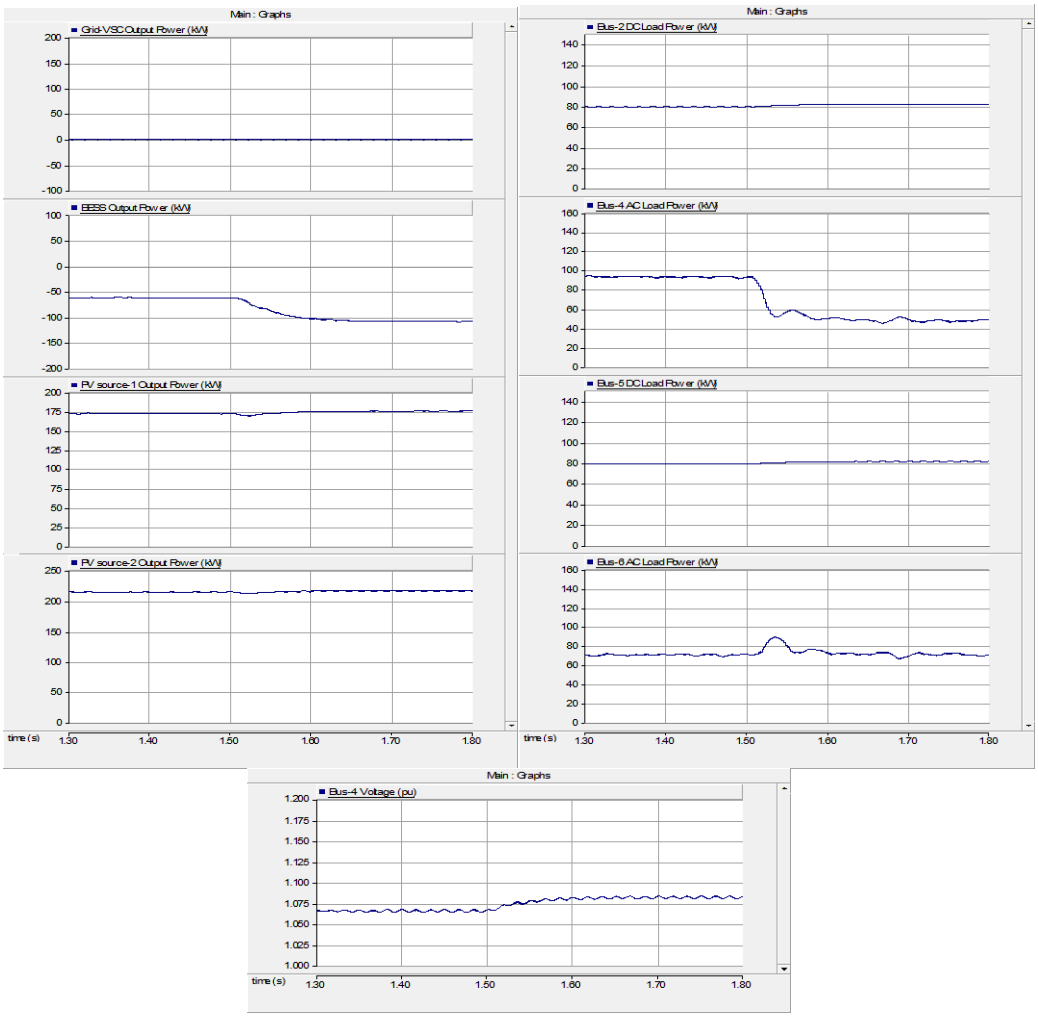

Figure 4.10: Simulation results of case 4.3.2.2

Table 4.3: Case 4.3.2.2 system voltages

Bus Number	1	2	3	4	5	6
Before	1.067	1.067	1.068	1.066	1.065	1.065
After	1.082	1.082	1.083	1.081	1.079	1.079

4.3.3 Change in Solar Irradiance

The system under study consists of two PV sources that normally operate in MPPT mode. A sudden change in solar irradiance such as that resulting from partial shading, for example, can cause an abrupt change in the power output by the PV source.

4.3.3.1 Grid-Connected Mode

In grid-connected mode, a change in the PV source output power should be compensated for from the utility. In case 4.3.3.1, the solar irradiance of PV source-1 was changed from 1000 W/m^2 to 750 W/m^2 at t = 0.5 sec. As can be seen in Figure 4.11 (a), this change caused a reduction in the power output by PV source-1from 160 kW to 120 kW. As a result, the power imported from the utility increased by 40 kW.

4.3.3.2 Isolated Mode

The results of case 4.3.3.2 are shown in Figure 4.11 (b). In this case, the solar irradiance of PV source-2 was changed from 1000 W/m^2 to 750 W/m^2 at t = 1.0 sec. As a result, the output power of PV source-2 was reduced from 213 kW to 159 kW. The BESS was controlling the voltage, so its charging power decreased from 63 kW to 11 kW due to the reduction in generation. The changes in system voltage for this case are shown in Table 4.4.

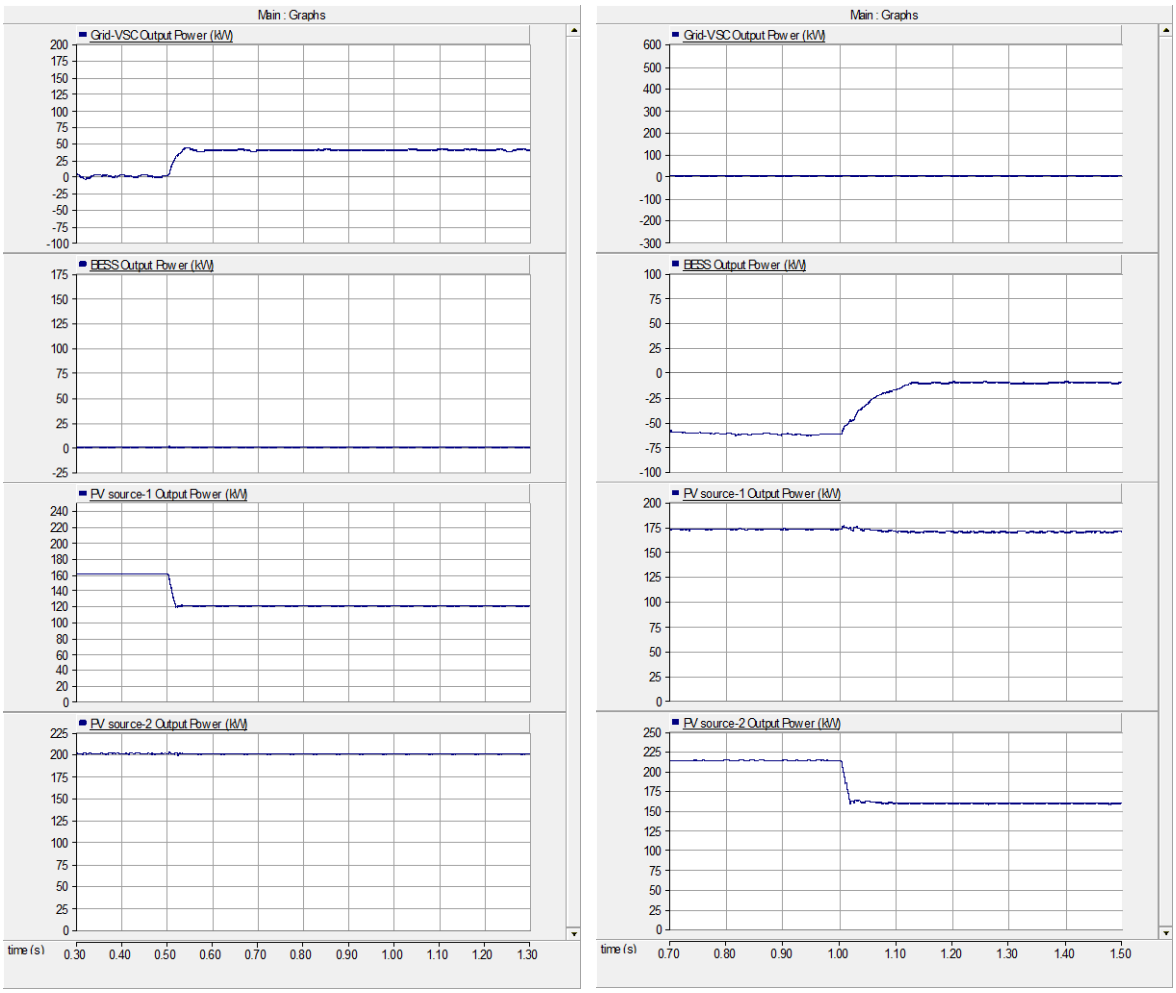

(a) **(b)**

Figure 4.11: Simulation results of cases 4.3.3.1 and 4.3.3.2

Table 4.4: System volages for case 4.3.3.2

Bus Number	1	2	3	4	5	6
Before	1.067	1.068	1.069	1.065	1.066	1.065
After	1.053	1.053	1.054	1.051	1.050	1.050

4.3.4 Microgrid Isolation from the Utility

Isolation from the utility is a fundamental feature of a microgrid that can occur intentionally or in emergency cases such as power outages in the utility network. Presented here are three scenarios of the control system reaction to microgrid isolation based on microgrid system loading and generation. Scenario 1 represents the case in which power is being exported to the utility at a rate less than the BESS charging rate. Scenario 2 represents the case in which power is being exported to the utility at a rate greater than the BESS charging rate. Scenario 3 represents the case in which power is being imported to the utility at a rate less than the BESS discharging rate. For all scenarios, the isolation of the microgrid is performed by opening the circuit breakers at the AC side of the grid-VSC, which is the isolation method typically used in DC systems for both normal and fault conditions [38]. The result is that the power exchanged by the grid-VSC gradually drops to zero after microgrid isolation which happens gradually due to the energy stored in the dc-side capacitor of the converter.

4.3.4.1 Microgrid Isolation Scenario 1

In this scenario, case 4.3.4.1, the total system loading is 225 kW, and the PV sources are assumed to be operating at rated powers of 160 kW and 200 kW. Microgrid isolation occurs at t = 0.5 sec, at which point the power exported to the utility is 131 kW, which is less than the BESS charging rate of 180 kW. As can be seen in Figure 4.12, the power exported by the grid-VSC drops to zero and the BESS reaches a charging rate of 138 kW after the isolation. BESS charging rate after isolation is higher than power exported to the utility before isolation because there is an increase in PV sources output powers as a result of the increase of their terminal voltages. Following the isolation, all system voltages are within voltage regulation limits, as shown in Table 4.5.

Table 4.5: System voltages for case 4.3.4.1

Bus Number	1	2	3	4	5	6
Before	1.001	1.002	1.004	1.001	1.000	0.999
After	1.090	1.090	1.091	1.090	1.088	1.087

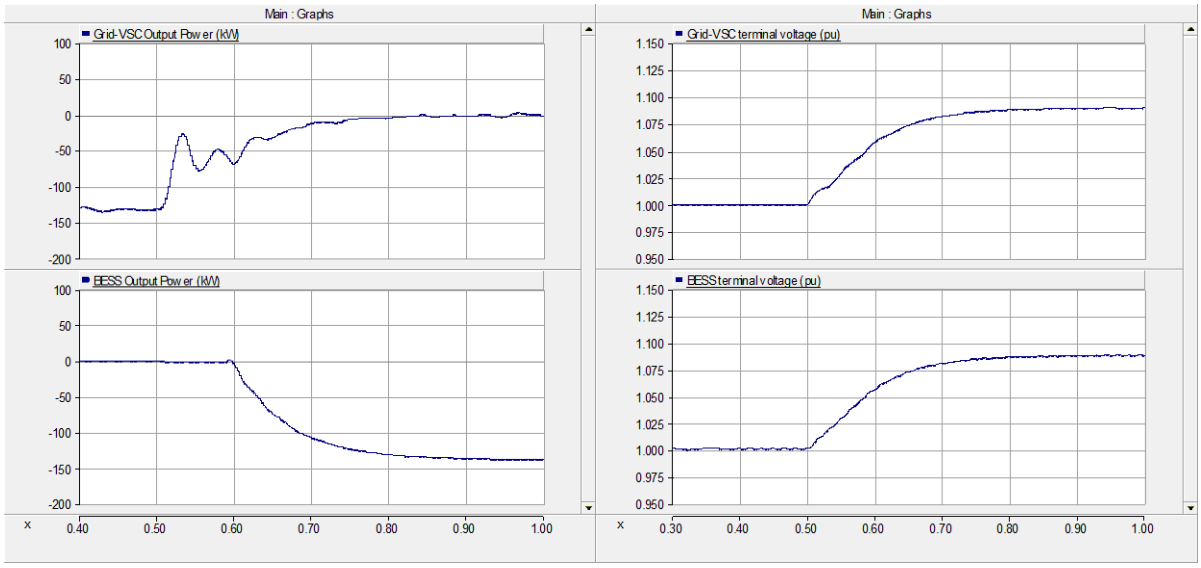

Figure 4.12: Simulation results of case 4.3.4.1

4.3.4.2 Microgrid Isolation Scenario 2

The total system loading in this scenario, case 4.3.4.2, is 88 kW, and the PV sources are also assumed to be supplying rated power. The microgrid was isolated at t = 0.5 sec, at which point 270 kW of power were exported to the utility, which is greater than the BESS charging rate. The BESS is therefore unable to prevent the voltage increase from exceeding the 1.1 per-unit upper voltage limit. The PV sources are therefore switched to adaptive control mode because the voltage at their terminals exceeds the 1.1 per-unit level.

As can be seen in Figure 4.13, the power exported by the grid-VSC drops to zero, and the BESS begins charging at a rate of 161 kW. At the same time, the output power of the PV sources is reduced from 160 kW and 200 kW to 112 kW and 154 kW, respectively. The voltage is also restored to within the voltage tolerance range through the shifting of the droop characteristics of the PV source controllers. The per-unit values of the power sharing between the two PV sources are 0.7 pu and 0.77 pu. This difference in power sharing values is attributable to the difference in voltage between the two buses where the PV sources are connected. Following isolation, all system voltages are within the voltage regulation limits, as shown in Table 4.6.

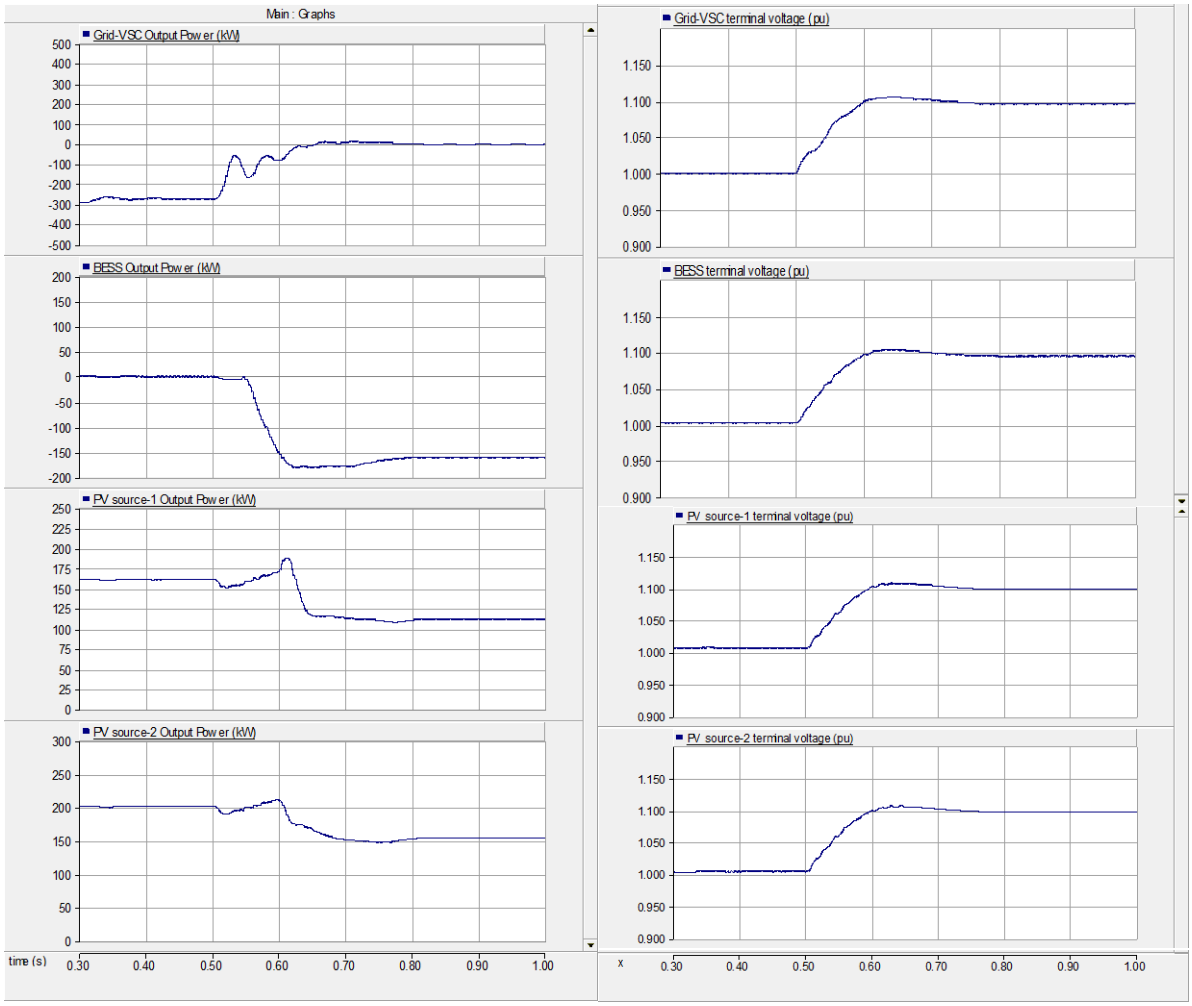

Figure 4.13: Simulation results of case 4.3.4.2

Table 4.6: System voltages for case 4.3.4.2

Bus Number	1	2	3	4	5	6
Before	1.003	1.004	1.006	1.005	1.002	1.002
After	1.096	1.097	1.098	1.097	1.095	1.095

4.3.4.3 Microgrid Isolation Scenario 3

In this scenario, case 4.3.4.3, the system was operating at a maximum loading of 360 kW. However the PV generation was reduced by changing the solar irradiance for both sources from 1000 W/m^2 to 800 W/m^2, resulting in the power deficit being imported from the utility. The microgrid was isolated from the utility at t = 0.5 sec, at which point 72 kW of power were imported from the utility, which is less than the BESS discharging rate. As can be seen in Figure 4.14, the power imported by the grid-VSC drops to zero, and the BESS reaches a discharging rate of 63 kW. Following the isolation, all system voltages are within the voltage regulation limits, as shown in Table 4.7.

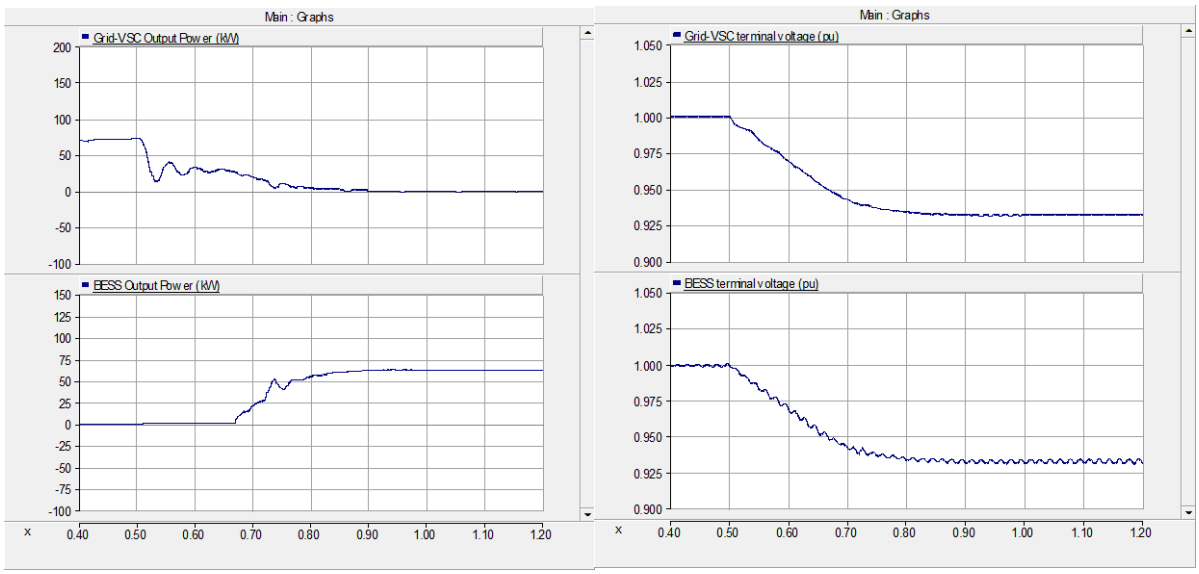

Figure 4.14: Simulation results of case 4.3.4.3

Table 4.7: System voltages for case 4.3.4.3

Bus Number	1	2	3	4	5	6
Before	1.000	0.999	1.000	1.000	0.999	0.998
After	0.932	0.933	0.933	0.934	0.932	0.931

4.3.5 Microgrid Reconnection to the Utility

When the cause of the isolation of the microgrid from the utility is cleared, the microgrid can be reconnected to the utility. Presented here are two scenarios for microgrid reconnection: the first scenario represents the case in which the PV sources are operating in MPPT control mode, and the second scenario represents the case in which the PV sources are operating in adaptive droop control mode.

4.3.5.1 Microgrid Reconnection Scenario 1

In this scenario, case 4.3.5.1, the microgrid was in isolated mode with the BESS controlling the voltage while charging at a rate of 138 kW. The microgrid was then reconnected to the utility at t = 1.0 sec. After the reconnection, the grid-VSC assumed constant voltage control of the DC voltage, and the voltage at its terminal was restored to a 1.0 per-unit level, as shown in Figure 4.15. As the voltage at the BESS terminal is returned to within ±5% of the nominal value, the BESS switches to standby mode with zero output power.

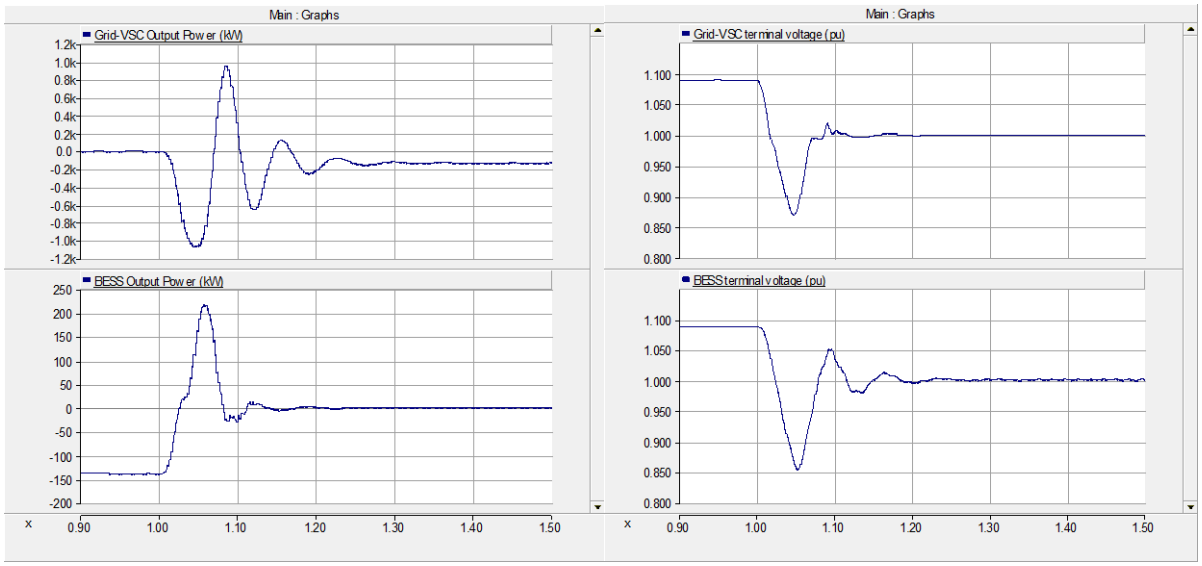

Figure 4.15: Simulation results of case 4.3.5.1

4.3.5.2 Microgrid Reconnection Scenario 2

In this scenario, case 4.3.5.2, the microgrid was in isolated mode with the BESS and PV sources controlling the voltage in droop control mode. After reconnection to the utility at t = 1.0 sec, voltage control was assumed by the grid-VSC, which regulated the voltage at its terminal to restore a 1.0 per-unit level, as shown in Figure 4.16. As the voltage at their terminals returned to within ±5% of the nominal value, the BESS switched to standby mode and the PV sources switched to MPPT control mode.

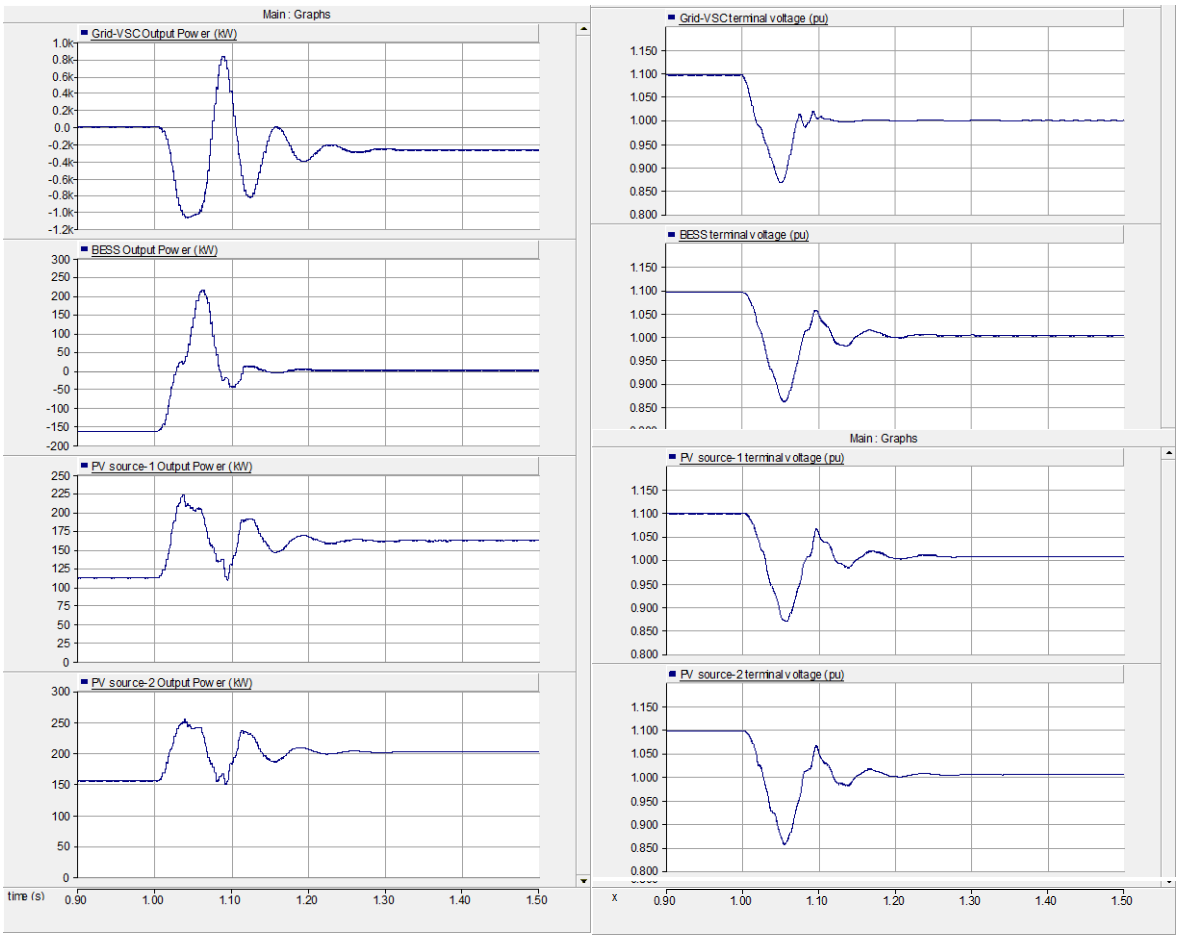

Figure 4.16: Simulation results of case 4.3.5.2

4.3.6 BESS SOC Limits

Based on the type of cells in the BESS, an upper state-of-charge (SOC) limit exists for battery charging, and a lower SOC limit exists for battery discharging. These limits are important with respect to prolonging the life of the battery. While the BESS is charging or discharging in microgrid isolated mode, there is a chance that one of these limits will be reached and that the BESS should therefore be isolated. The results for one case, case 4.3.6, are presented here, in which the BESS reaches its upper SOC limit, assumed to be an 80% SOC.

As can be seen in Figure 4.17, the BESS was charging at a 161 kW rate until it reached a maximum SOC limit of 80% at t = 1.32 sec. The BESS was therefore isolated, and as a result, the power output from the PV sources was reduced from 141 kW and 184 kW to 72 kW and 89 kW, respectively.

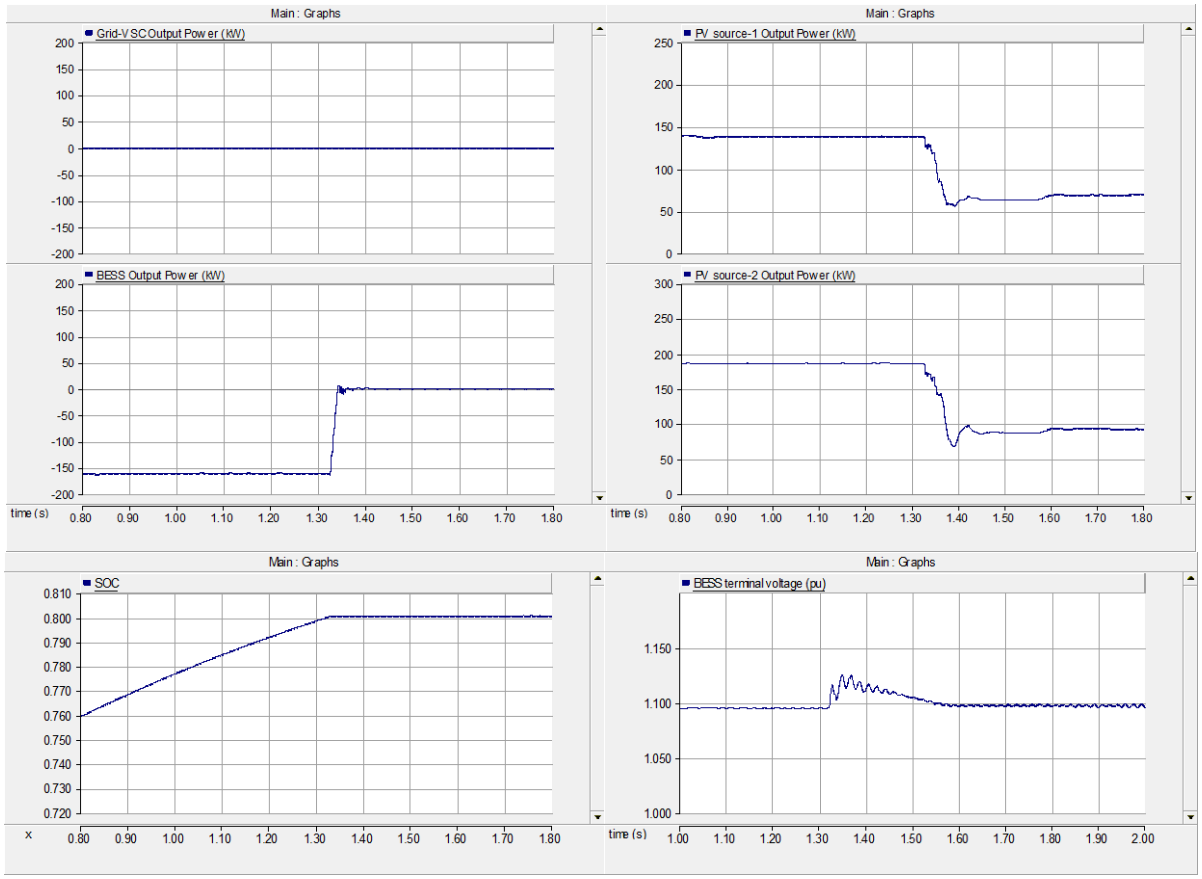

Figure 4.17: Simulation results of case 4.3.6

4.4 Discussion

A power control strategy has been implemented as part of the developed low-voltage DC microgrid model. An autonomous distributed strategy has been utilized because, in this type of strategy, control is provided by several converters and involves no communication between the controllers. The coordination of the controllers is achieved through the use of the DC voltage as a signal for identifying the operating mode of the system since a steady DC voltage indicates that power balance has been achieved in the DC microgrid. The DC voltage tolerance used in this work is a deviation of ±5% from the nominal value for grid-connected mode and ±10% from the nominal value for isolated mode.

The control strategy is based on a five-operating-mode control strategy previously proposed in the literature. However, in this work, the control strategy was modified in order to maximize the utilization of renewable energy by allowing renewable PV sources to continue operating in MPPT mode until the voltage tolerance limit is violated. When the upper voltage tolerance limit is exceeded, the DG converters then switch to droop control mode in order to limit the increase in system voltage by curtailing the power output by the renewable energy sources.

The use of a fixed droop characteristic for PV converters can limit increases in system DC voltages but cannot restore system voltages to an acceptable voltage range. An adaptive droop characteristic is therefore proposed in this work, whereby the droop curve of the PV converters is changed as the voltage exceeds the upper voltage tolerance limit in order to bring the voltage back within an acceptable range. This is achieved through shifting down the droop curve gradually until the voltage at the PV converter terminal becomes less than the 1.1 per-unit level.

The functionality of the power control strategy has been verified using PSCAD power system simulator. The simulation case studies include normal system operation with the maximum load, sudden changes in generation or loading, and microgrid isolation from and reconnection to the utility under a variety of operating conditions. In grid-connected mode, the grid-VSC absorbs any sudden increase in generation and compensates for any sudden change in loading in order to maintain the voltage at its terminal at a 1.0 per-unit level, as

illustrated by cases 4.3.2.1 and 4.3.3.1. However, in isolated mode, the BESS converter assumes this role by charging or discharging the battery to maintain the power balance in the system, as illustrated by cases 4.3.2.2 and 4.3.3.2. For all cases, system voltages are maintained within the voltage tolerance limits. Changes in the system voltages are smaller in grid-connected mode than in isolated mode since constant voltage control is used for the grid-VSC, while droop control is used for the BESS converter.

Intentional or emergency microgrid isolation from the utility can occur during different microgrid operating conditions. For this reason, three scenarios were employed as representations of different system loading and generation levels. Cases 4.3.4.1 and 4.3.4.3 constitute examples of microgrid isolation when the power exchanged with the utility is less than the BESS charging or discharging rate. In both cases, the BESS converter switched from standby to droop control mode as the voltage at the BESS terminal exceeded a deviation of ±5% from the nominal voltage. The BESS then supplied or absorbed the amount of power required to maintain the power balance in the system. Following isolation, all of the system voltages were maintained within the ±10% voltage tolerance limits for isolated mode. Case 4.3.4.2 represents microgrid isolation when the power exchanged with the utility exceeds the BESS charging rate. In this case, the charging power of the BESS converter failed to limit the voltage increase, so the DC voltage exceeded the +10% upper voltage tolerance limit in isolated mode. The PV source converters therefore switched to adaptive droop control mode in order to limit the voltage increase by curtailing the output power of the PV sources. At the same time, the droop characteristics of the PV converters were altered to return the voltages at the converter terminals to within a ±10% deviation from the voltage tolerance limits for isolated mode.

Two further scenarios were considered with respect to the reconnection of the microgrid to the utility. Case 4.3.5.1 represents microgrid reconnection when the PV sources are operating in MPPT mode, and case 4.3.5.2 represents microgrid reconnection when the PV sources are operating in adaptive droop control mode. In both cases, the grid-VSC restored the constant voltage control of the system by regulating the voltage at its terminal so that it returned to a 1.0 per-unit level. As the voltages at the BESS and PV source terminals

were brought back to within the ±5% voltage tolerance limits for grid-connected mode, the BESS converter switched to standby mode, and the PV converters switched to MPPT control mode.

BESS reaching its charging or discharging SOC limits are likely occurrences for microgrid isolated modes of operation. Case 4.3.6 represents the case when BESS reaches its upper SOC limit as a result of charging the storage system with surplus power delivered by PV sources. Upon reaching the limit, BESS was isolated and the output power of PV sources was curtailed in order to maintain the power balance in the microgrid.

Power sharing between DGs is an important aspect discussed in literature for microgrids with multiple DG units. The two PV sources in the system under study normally operate in MPPT mode where no power sharing mechanism is needed. When PV sources operate in adaptive droop mode, the power sharing between PV sources is designed to be proportional to their rated powers. This is implemented through selecting the droop constant of each PV source to be proportional to its rated power. However, since the PV sources are connected to different system buses, a small mismatch occurred in the power sharing due to the difference in the bus voltages as shown in cases 4.3.4.2 and 4.3.6. Precise power sharing between the PV sources can be achieved by using the average of their bus voltages in their control schemes. However this would require real-time exchange of bus voltages values through a communication means while autonomous control scheme is desirable for this work.

The simulation results verified the functionality of the power control strategy during different microgrid modes of operation and a variety of system perturbations such as modes transitions, and sudden generation and loading changes.

Chapter 5

Conclusions and Future Work

5.1 Conclusions

A DC microgrid represents a promising concept that has the potential to improve power system reliability and stability. A number of research groups around the world are investigating this concept with the use of simulation platforms and experimental setups. PSCAD power system simulator was used in this work for the modeling and simulation of a DC microgrid. PSCAD contains many ready-to-use models of power system devices and controllers, and as reported in the literature, has proven to be a powerful tool for simulating the performance of power system elements and their control algorithms.

Several methods have been proposed for the power management of DC microgrids: hierarchical, distributed, and intelligent control strategies. Ongoing research is directed at optimizing these techniques for DC microgrid application. In this work, an autonomous distributed control strategy has been implemented as a means of ensuring voltage regulation and seamless microgrid isolation. The coordination of a variety of system controllers has been achieved using the DC system voltage as a signal for identifying the operating state of the system. This autonomous strategy improves system reliability since it avoids reliance on a central controller or communication links. The expandability of the microgrid is also

facilitated because the introduction of additional DG does not require modifications to the existing controllers.

An adaptive droop control technique has been proposed for PV source converters in order to maximize the utilization of the power available from these sources while ensuring the regulation of the system voltage. This technique allows PV sources to continue to operate MPPT control mode until the voltage regulation limit is violated. When the limit is exceeded, controllers curtail the output power of the PV sources and, at the same time, restore the PV terminal voltages to within the tolerance range. An additional feature is the selection of droop constants that correlate with the rated power allowed for proportional power sharing between the PV sources. However, since the PV sources are connected to different system buses, a small mismatch occurred in the power sharing due to the difference in the bus voltages.

5.2 Future Work

As a continuation of the work conducted for this thesis, suggestions for future research include the following:

- Investigate the economics of using battery energy storage systems (BESSs) for voltage regulation in microgrid isolated mode of operation. The investigation should include consideration of the role of the storage system in saving the renewable energy available for future use.
- Implement an SOC management control for battery energy storage system in grid-connected mode.
- Develop an automatic load-shedding scheme for load converters in order to reduce system loading during periods of low availability of energy from renewable and energy storage sources. A low power supply can be detected autonomously through the monitoring of the DC voltage of the system.
- Study power system protection for DC systems and power electronic converters with respect to fault detection and isolation.

References

[1] B. Kroposki, R. Lasseter, T. Ise, S. Morozumi, S. Papatlianassiou, and N. Hatziargyriou, "Making Microgrids Work," *Power Energy Mag. IEEE*, vol. 6, no. 3, pp. 40–53, 2008.

[2] N. Hatziargyriou, H. Asano, R. Iravani, and C. Marnay, "Microgrids: An Overview of Ongoing Research , Development , and Demonstration Projects," *IEEE Power Energy Mag.*, pp. 78–94, 2007.

[3] R. H. Lasseter and P. Paigi, "Microgrid: a Conceptual Solution," in *IEEE 35th Annual Power Electronics Specialists Conference*, 2004, pp. 4285–4290.

[4] K. A. Nigim and W.-J. Lee, "Micro Grid Integration Opportunities and Challenges," in *IEEE Power Engineering Society General Meeting*, 2007, pp. 1–6.

[5] Q. Zhong, L. Lin, Y. Zhang, and Z. Wu, "Study on the Control Strategies and Dynamic Performance of DC Distribution Network," in *IEEE Power and Energy Society General Meeting*, 2012, pp. 1–5.

[6] D. Chen and L. Xu, "Autonomous DC Voltage Control of a DC Microgrid With Multiple Slack Terminals," *IEEE Trans. Power Syst.*, vol. 27, no. 4, pp. 1897–1905, 2012.

[7] S. Anand, B. G. Fernandes, and J. Guerrero, "Distributed Control to Ensure Proportional Load Sharing and Improve Voltage Regulation in Low-Voltage DC Microgrids," *IEEE Trans. Power Electron.*, vol. 28, no. 4, pp. 1900–1913, Apr. 2013.

[8] J. Li, X. Zhang, and W. Li, "An Efficient Wind-Photovoltaic Hybrid Generation System For Dc Micro-Grid," in IET *8th International Conference on Advances in Power System Control, Operation and Management*, 2009, pp. 1–6.

[9] B. K. Johnson and R. H. Lasseter, "An Industrial Power Distribution System Featuring Ups Properties," in *Power Electronics Specialists Conference*, 1993, pp. 759 – 765.

[10] Z. H. Jian, Z. Y. He, J. Jia, and Y. Xie, "A Review of Control Strategies for DC Micro-grid," in *Fourth International Conference on Intelligent Control and Information Processing*, 2013, pp. 666–671.

[11] J. M. Guerrero, J. C. Vasquez, J. Matas, L. G. De Vicuña, and M. Castilla, "Hierarchical Control of Droop-Controlled AC and DC Microgrids — A General Approach Toward Standardization," *IEEE Trans. Ind. Electron.*, vol. 58, no. 1, pp. 158–172, 2011.

[12] L. Zhang, T. Wu, Y. Xing, K. Sun, and J. M. Gurrero, “Power Control of DC Microgrid Using DC Bus Signaling,” in *IEEE Applied Power Electronics Conference and Exposition (APEC)*, 2011, pp. 1926–1932.

[13] D. Chen, L. Xu, and L. Yao, “DC Voltage Variation Based Autonomous Control of DC Microgrids,” *IEEE Trans. Power Deliv.*, vol. 28, no. 2, pp. 637–648, 2013.

[14] T. Logenthiran, D. Srinivasan, A. Khambadkone, and H. N. Aung, “Multiagent System for Real-Time Operation of a Microgrid in Real-Time Digital Simulator,” *IEEE Trans. Smart Grid*, vol. 3, no. 2, pp. 925–933, 2012.

[15] C. Yoo, W. Choi, I. Chung, D.-J. Won, S.-S. Hong, and B.-J. Jang, “Hardware-In-the-Loop Simulation of DC Microgrid with Multi-Agent System for Emergency Demand Response,” in *Power and Energy Society General Meeting*, 2012, pp. 1–6.

[16] H. Kakigano, A. Nishino, and T. Ise, “Distribution Voltage Control for DC Microgrid with Fuzzy Control and Gain-Scheduling Control,” in *8th International Conference on Power Electronics - ECCE Asia*, 2011, pp. 725 – 730.

[17] P. Thounthong, S. Sikkabut, A. Luksanasakul, P. Koseeyaporn, P. Sethakul, S. Pierfederici, and B. Davat, “Fuzzy Logic Based DC Bus Voltage Control of a Stand Alone Photovoltaic/Fuel Cell/Supercapacitor Power Plant,” in *11th International Conference on Environment and Electrical Engineering*, 2012, pp. 725 – 730.

[18] D. M. Tagare, *Electric Power Generation: The Changing Dimensions*. the Institute of Electrical and Electronics Engineers, Inc., 2011, pp. 195–216.

[19] V. Quaschning, *Renewable Energy and Climate Change*. Wiley-IEEE Press, 2010, pp. 144–164.

[20] X. Sun, Z. Lian, B. Wang, and X. Li, “A Hybrid Renewable DC Microgrid Voltage Control,” in *IEEE 6th International Power Electronics and Motion Control Conference*, 2009, vol. 3, pp. 725–729.

[21] B. Wang, M. Sechilariu, and F. Locment, “Intelligent DC Microgrid With Smart Grid Communications: Control Strategy Consideration and Design,” *IEEE Trans. Smart Grid*, vol. 3, no. 4, pp. 2148–2156, 2012.

[22] F. Ferret and M. Simões, *Integration of Alternative Sources of Energy: Storage Systems*. Wiley-IEEE Press, 2006, pp. 262–300.

[23] H. Kakigano, Y. Miura, T. Ise, and R. Uchida, “DC Micro-grid for Super High Quality Distribution - System Configuration and Control of Distributed Generations and Energy Storage Devices -,” in *Power Electronics Specialists Conference*, 2006, pp. 1–7.

[24] H. Kakigano, Y. Miura, and T. Ise, “Low-Voltage Bipolar-Type DC Microgrid for Super High Quality Distribution,” *IEEE Trans. Power Electron.*, vol. 25, no. 12, pp. 3066–3075, Dec. 2010.

[25] S. Grillo, V. Musolino, L. Piegari, E. Tironi, and C. Tornelli, “DC Islands in AC Smart Grids,” *IEEE Trans. Power Electron.*, vol. 29, no. 1, pp. 89–98, Jan. 2014.

[26] J. Stevens and B. Schenkman, “DC Energy Storage in the CERTS Microgrid.” Sandia National Laboratories, 2008.

[27] K. Kurohane, T. Senjyu, Y. Yonaha, A. Yona, T. Funabashi, and C. Kim, “A Distributed DC Power System in an Isolated Island,” in *IEEE International Symposium on Industrial Electronics*, 2009, no. ISlE, pp. 1–6.

[28] L. Xu and D. Chen, “Control and Operation of a DC Microgrid With Variable Generation and Energy Storage,” *IEEE Trans. Power Deliv.*, vol. 26, no. 4, pp. 2513–2522, 2011.

[29] O. Tremblay, L.-A. Dessaint, and A.-I. Dekkiche, “A Generic Battery Model for the Dynamic Simulation of Hybrid Electric Vehicles,” in *IEEE Vehicle Power and Propulsion Conference*, 2007, no. V, pp. 284–289.

[30] J.-D. Park, “Simple Flywheel Energy Storage using Squirrel-cage Induction Machine for DC Bus Microgrid Systems,” in *IEEE Industrial Electronics Society Conference*, 2010, pp. 3040–3045.

[31] K. W. Hu and C. M. Liaw, “On the Flywheel/Battery Hybrid Energy Storage System for DC Microgrid,” in *Future Energy Electronics Conference*, 2013, pp. 119–125.

[32] T. Karaipoom and I. Ngamroo, “Enhancement of LVRT Performance and Alleviation of Power Fluctuation of DFIG Wind Turbine in DC Microgrid by SMES,” in *IEEE International Conference on Applied Superconductivity and Electromagnetic Devices*, 2013, vol. 5, pp. 207–208.

[33] J. Eto, R. Lasseter, B. Schenkman, J. Stevens, D. Klapp, H. Volkommer, E. Linton, H. Hurtado, and J. Roy, “Overview of the CERTS Microgrid Laboratory Test Bed.” CIGRE, 2009.

[34] D. Fregosi, S. Bhattacharya, and S. Atcitty, “Empirical Battery Model Characterizing a Utility-scale Carbon-enhanced VRLA Battery,” in *IEEE Energy Conversion Congress and Exposition*, 2011, pp. 3541–3548.

[35] S. Liu and R. A. Dougal, “Dynamic Multiphysics Model for Solar Array,” *IEEE Trans. Energy Convers.*, vol. 17, no. 2, pp. 285–294, 2002.

[36] “PSCAD/EMTDC Power System Simulation Software User Manual: Photovoltaic Source.” Manitoba HVDC Research Center, Manitoba, Canada, 2012.

[37] A. Yazdani and R. Iravani, *Voltage-Sourced Converters in Power Systems*. Wiley-IEEE Press, 2010.

[38] J. Park and J. Candelaria, “Fault Detection and Isolation in Low-Voltage DC-Bus Microgrid System,” *IEEE Trans. Power Deliv.*, vol. 28, no. 2, pp. 779–787, 2013.